only clearly observed in the presence of the ODN with the target cytidine, which suggests that the activation is dependent on cytidine.

The biological stability of the ODNs was investigated in a cell lysate and in the presence of DNase I. It was shown that the modified ODN **6A** (X = AP, R^2 = SMe) was slightly more stable than the natural ODN **6A** (X = G), and that the PEG conjugate **8A** (X = G) exhibits high stability in a cell lysate (Figure 2a). To rule out the possibility that the higher activity

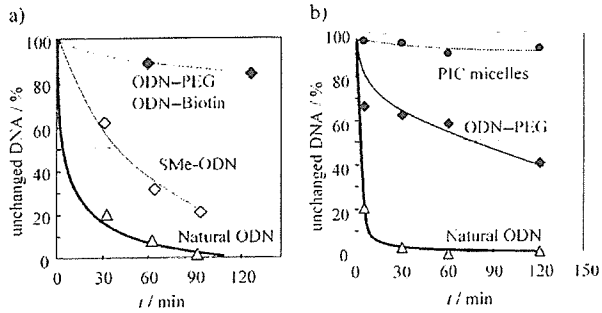

Figure 2. Comparison of the stability of the ODN derivatives in a cell lysate (a) and in the presence of DNase I (b) at 30 °C. Natural ODN: **6A** (X = G), SMe-ODN: **6A** (X = AP, R^2 = SMe), ODN–PEG: **8A** (X = G), ODN–biotin: biotin amide of **5A** (X = G), PIC micelles: B-PEI + **8A** (X = G) (N/P = 1; B-PEI: M_w = 25000, DP = 580). B-PEI = branched polyethyleneimine, DP = degree of polymerization.

of the modified ODNs is merely an effect of higher biostability induced by the modification, we next investigated the antisense effect of the PEG conjugates. The ODN–PEG conjugates were incubated with mRNA of firefly luciferase for 30 min in a buffer, and translation was performed by treatment with an amino acid mixture in a cell lysate for 90 min at 30 °C. It was clearly demonstrated that the PEG conjugate with the modified ODN, **8A** (X = 2AP, R^2 = SMe), exhibited a higher inhibitory effect than the conjugate with the natural ODN, **8A** (X = G), and that the biostability of the modified ODN is not a major factor in the enhancement of the antisense effect.[25]

Hybridization of the ODN with the luciferase mRNA following a cross-linking reaction was next investigated by reverse-transcription polymerase chain reaction (RT-PCR). When primers were used for the upstream and downstream regions of the antisense target site, it was expected that the PCR with cross-linked mRNA would produce shorter PCR products than that with unmodified mRNA. First, ODN **6A** (X = G or 2AP, R^2 = SPh) was mixed with mRNA in a buffer, the mixture was subjected to RT-PCR, and the products were analyzed by gel electrophoresis (Figure 3). The RT-PCR products corresponding to a 223-mer nucleotide of the full length were formed as the major product (Figure 3, lanes 2 and 3), thus indicating that neither covalent nor noncovalent hybridized complexes were formed effectively in a buffer. We next attempted to form complexes with mRNA in cell lysates, so that we could isolate the complexes by using streptavidin affinity beads. mRNA and biotin-conjugated ODN were incubated in a cell lysate, and the hybridized complexes were separated with streptavidin beads. (**5A**–biotin is as biostable

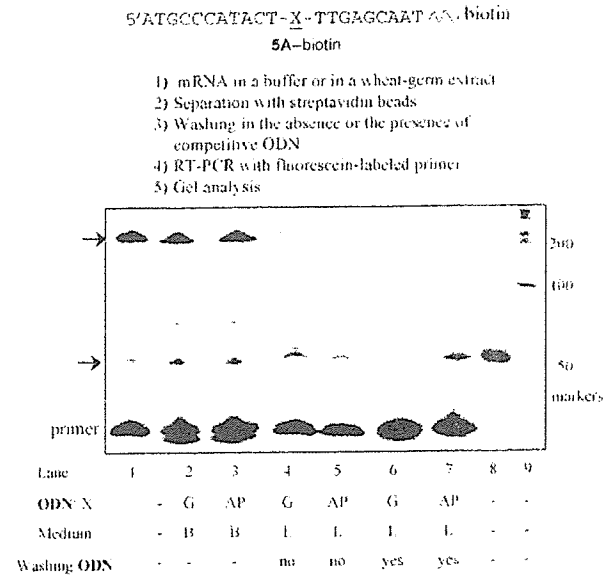

Figure 3. Analysis of RT-PCR products (denoted by arrows) of the reaction of the ODN and luciferase mRNA. Lane 1: control; lane 2: ODN **6A** (X = G) and mRNA were subjected to RT-PCR; lane 3: ODN **6A** (X = 2AP, R^2 = SPh) was used in the same procedure as that for lane 2; lane 4: ODN **5A**–biotin (X = G) and mRNA complexes were separated with streptavidin beads then washed several times with a buffer in the absence of the competitive ODN; lane 5: ODN **5A**–biotin (X = 2AP, R^2 = SPh) was used in the same procedure as that for lane 4; lane 6: washing was done in the presence of the competitive ODN in otherwise the same procedure as that used for lane 4; lane 7: washing was done in the presence of the competitive ODN in otherwise the same procedure as that used for lane 5; lanes 8 and 9: markers. G is guanosine and AP is 2-amino-6-(2-phenylthioethyl)purine (R^2 = SPh; see Scheme 2). Medium B is a buffer and medium L is lysate. The ODN **5A**–biotin has a biotin unit at its 3′ amino end. The sequence of the washing ODN (21 mer) is the sense sequence 3′-TACGGCTATGA-C-AACTCGTTA-5′: the target sequence of firefly-luciferase mRNA.

as the ODN–PEG conjugate, as shown in Figure 2a.) The PCR in which separated streptavidin beads were used afforded shorter RT-PCR products of approximately 50-mer length (Figure 3, lanes 4 and 5), which showed that the RT reaction was inhibited before the site of cross-linking with both the natural ODN (X = G) and the cross-linking ODN (X = 2AP, R^2 = SPh). These results also clearly indicate that tight ODN–mRNA complexes are formed in cell lysates, but not in a buffer, in the case of both the natural and the modified ODN. When the separated streptavidin beads were washed in the presence of the competitive ODN, the short RT-PCR products disappeared in lane 6 and were retained in lane 7, thus demonstrating that covalently bound ODN–mRNA complexes are formed with the cross-linking ODN (X = 2AP, R^2 = SPh). These results, together with the fact that the sulfide derivative is transformed into a 2-amino-6-vinylpurine derivative in cell lysates,[25] strongly suggest that the ODN with the reactive 2-aminopurine residue forms the covalent bond with the target mRNA in the cell lysate to enhance the antisense effect.

We next evaluated the intracellular antisense activity of the reactive ODN–PEG conjugates by a dual-luciferase-

reporter assay. The PIC micelles of the reactive ODN–PEG conjugates exhibit high stability toward enzymatic digestion (Figure 2b) and were therefore used as the system for the delivery of the ODN into the cellular interior.[21,22,25] HuH-7 cells were cotransfected with plasmids of firefly and renilla luciferases in amounts at which both luciferases are expressed to a similar extent. The cells were incubated for 24 h in the presence of the reactive ODN–PEG as the PIC micelles and then for 24 h in a fresh medium. The PEG–ODN conjugates were mixed with PLL (poly-L-lysine, DP = 100, M_w = 20900) with a 1:1 molar ratio of the phosphate group in the PEG–ODN conjugate and the amino group in PLL (N/P = 1) to form the PIC micelles. The luciferase expression was monitored by measuring luminescence with the dual luciferase assay kit. Antisense effects are summarized in Figure 4.

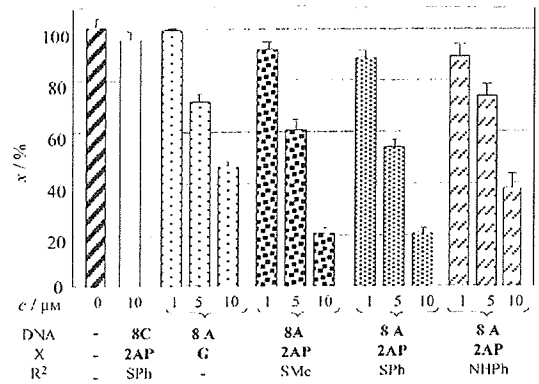

Figure 4. Antisense effects with PEG–ODN/PLL PIC micelles against gene expression of firefly luciferase in cultured HuH-7 cells. Normalized ratios x of firefly-luciferase activity to that of renilla luciferase are shown in the ordinate. G and 2AP represent guanosine and the 2-amino 6-alkyl purine nucleoside; substituents R^2 are shown in Scheme 2.

Neither the antisense ODN **6A** nor the PEG–ODN **8A** alone showed antisense inhibition.[21,22] Under conditions under which the PIC micelles of the PEG–ODN **8C** with the random sequence did not show an antisense effect, the micelles of the natural PEG–ODN **8A** clearly showed potent antisense effects of about 50% inhibition at 10 μM. Although higher concentrations of the PIC micelles were needed for potent inhibition than those required in the antisense experiments in cell lysates (compare Figures 1 and 4), the PIC micelles formed with the ODN–PEG conjugates and PLL did not cause cytotoxicity at concentrations of 10 μM.[25] Thus, the inhibitory effects summarized in Figure 4 result from selective antisense effects of **8A**. The sulfide derivatives of 2-aminopurine (**8A**, X = AP, R^2 = SMe and SPh) showed greater antisense effects than the PEG conjugate with the natural antisense oligonucleotide (**8A**, X = G). At a concentration of 10 μM in the sulfide derivative, luciferase expression was inhibited to 20% of that in the control. This degree of expression corresponds to a background level. The ODN containing the aniline derivative (**8A**, X = AP, R^2 = NHPh) was used as an unreactive antisense control. In the presence of this ODN, less effective antisense inhibition was observed, which again supports the hypothesis that the 2-aminopurine derivative in the reactive ODN enhances antisense inhibition.

The consequences of one mismatched site on the antisense effects are compared in Figure 5 for the natural antisense

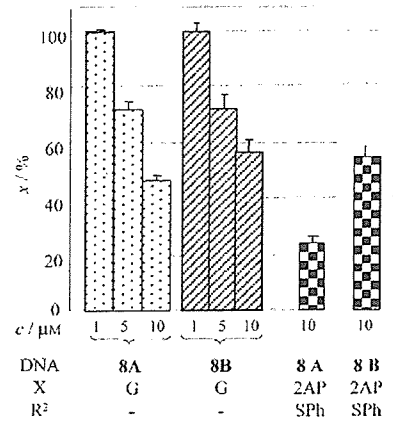

Figure 5. Comparison of the consequences of one mismatched site on the antisense effects. Systems were assayed for their antisense effect in a similar way to that described in the footnote of Figure 4. G and 2AP represent guanosine and the 2-amino 6-alkyl purine nucleoside; substituents R^2 are shown in Scheme 2. x = normalized ratios of firefly-luciferase activity to that of renilla luciferase. Target mRNA sequence: -3'-TACGGGTATGA-C-AACTCGTTA-; antisense sequences: **8A**: 5'-ATGCCCATACT-X-TTGAGCAAT-PEG, **8B**: 5'-ATGCCCATACT-G-XTGAG-CAAT-PEG.

ODNs (**8A** and **8B**, X = G) and the reactive ODNs (**8A** and **8B**, X = 2AP, R^2 = SPh). The natural ODN with one mismatched site (**8B**, X = G) exhibited similar inhibition to that of the fully matched ODN (**8A**, X = G), which demonstrates a disadvantage to the use of natural ODNs in terms of antisense inhibition. In marked contrast, the reactive ODN (**8B**, X = AP, R^2 = SPh), in which the 2-aminopurine derivative is at the position adjacent to the target cytidine, was much less efficient than the fully matched ODN (**8A**, X = AP, R^2 = SPh), thus demonstrating the superiority of the reactive ODN over the natural antisense ODN in discriminating a single nucleoside difference in cells. As the 2-amino-6-(2-phenylthioethyl)purine nucleoside is highly selective to cytidine at the complementary position,[17,18] the high sensitivity to a single mismatch site can also be reasonably interpreted as a result of selective cross-linking with the 2-amino-6-vinylpurine derivative.

In this study, we have applied the inducible alkylating system that has been developed by our research group to intracellular antisense oligonucleotides. It was found that the sulfide derivative of the 2-amino-6-vinylpurine nucleoside exhibited high reactivity in a cell lysate, in striking contrast to the chemical reactivity investigated in simple model systems. Detailed investigations of the reaction product of the reactive ODN with mRNA in a cell lysate strongly suggest that the reactive ODN that incorporates the 2-aminopurine nucleoside analogue forms a covalent bond with the target mRNA. The reactive ODN was subsequently applied in intracellular antisense inhibition of luciferase by using polyion-complex

(PIC) micelles of the PEG–ODN conjugate. In conclusion, we have successfully shown that the inducible alkylation system functions in an intracellular environment to promote efficient and selective antisense activity against luciferase production. A unique benefit of this alkylating agent is reflected in its high selectivity, which may permit the discrimination of a single nucleotide difference in cells. As the sulfide precursors to the 2-amino-6-vinylpurine derivative, unlike psoralen, do not need UV irradiation for activation, they are expected to be useful for further in vivo applications. This type of inducible alkylation system combined with the delivery system of PIC micelles for PEG conjugates opens new opportunities for the use of reactive oligonucleotides in vivo.

Received: December 14, 2005
Revised: February 3, 2006
Published online: March 30, 2006

Keywords: alkylation · antisense oligonucleotides · biological chemistry · cross-linking · inducible reactivity

[1] K. B. Grant, P. B. Dervan, *Biochemistry* **1996**, *35*, 12313–12319.
[2] For a recent review, see: S. Sasaki, *Eur. J. Pharm. Sci.* **2001**, *13*, 43–51; see also references therein.
[3] Q. B. Zhou, S. E. Rokita, *Proc. Natl. Acad. Sci. USA* **2003**, *100*, 15452–15457.
[4] Y. Yamamoto, W. Tsuboi, M. Komiyama, *Nucleic Acids Res.* **2003**, *31*, 4497–4502.
[5] T. Fukuma, C. M. Walton, C. H. Wu, G. Y. Wu, *Bioconjugate Chem.* **2003**, *14*, 295–301.
[6] R. N. Zuckermann, D. R. Corey, P. G. Schultz, *J. Am. Chem. Soc.* **1988**, *110*, 1614–1615.
[7] K. Nagai, S. M. Hecht, *J. Biol. Chem.* **1991**, *266*, 23994–24002.
[8] S. Sando, H. Abe, E. T. Kool, *J. Am. Chem. Soc.* **2004**, *126*, 1081–1087.
[9] M. P. van de Corput, R. W. Dirks, R. P. M. van Gijlswijk, E. van Binnendijk, C. M. Hattinger, R. A. de Paus, J. E. Landegent, A. K. Raap, *J. Histochem. Cytochem.* **1998**, *46*, 1249–1259.
[10] G. Meister, M. Landthaler, Y. Dorsett, T. Tuschl, *RNA* **2004**, *10*, 544–550.
[11] G. Hutvagner, M. J. Simard, C. C. Mello, P. D. Zamore, *PLoS Biol.* **2004**, *2*, e98.
[12] A. Murakami, A. Yamayoshi, R. Iwase, J. Nishida, T. Yamaoka, N. Wake, *Eur. J. Pharm. Sci.* **2001**, *13*, 25–34.
[13] J. M. Kean, A. Murakami, K. R. Blake, D. D. Cushman, P. S. Miller, *Biochemistry* **1988**, *27*, 9113–9121.
[14] N. Puri, A. Majumdar, B. Cuenoud, P. S. Miller, M. M. Seidman, *Biochemistry* **2004**, *43*, 1343–1351.
[15] A. Majumdar, A. Khorlin, N. Dyatkina, F. L. Lin, J. Powell, J. Liu, Z. Fei, Y. Khripine, K. A. Watanabe, J. George, P. M. Glazer, M. M. Seidman, *Nat. Genet.* **1998**, *20*, 212–214.
[16] Q. B. Zhou, S. E. Rokita, *Proc. Natl. Acad. Sci. USA* **2003**, *100*, 15452–15457.
[17] T. Kawasaki, F. Nagatsugi, Md. M. Ali, M. Maeda, K. Sugiyama, K. Hori, S. Sasaki, *J. Org. Chem.* **2005**, *70*, 14–23.
[18] F. Nagatsugi, T. Kawasaki, D. Usui, M. Maeda, S. Sasaki, *J. Am. Chem. Soc.* **1999**, *121*, 6753–6754.
[19] F. Nagatsugi, K. Uemura, S. Nakashima, M. Maeda, S. Sasaki, *Tetrahedron* **1997**, *53*, 3035–3044.
[20] F. Nagatsugi, K. Uemura, S. Nakashima, M. Maeda, S. Sasaki, *Tetrahedron Lett.* **1995**, *36*, 421–424.
[21] M. Oishi, S. Sasaki, Y. Nagasaki, K. Kataoka, *Biomacromolecules* **2003**, *4*, 1426–1432.
[22] M. Oishi, F. Nagatsugi, S. Sasaki, Y. Nagasaki, K. Kataoka, *ChemBioChem* **2005**, *6*, 1–6.
[23] For a similar method, see: J. H. Jeong, S. W. Kim, T. G. Park, *Bioconjugate Chem.* **2003**, *14*, 473–479.
[24] M. Mishra, J. R. Bennett, G. Chaudhuria, *Biochem. Pharmacol.* **2001**, *61*, 467–476.
[25] See the Supporting Information.

pH-Responsive Three-Layered PEGylated Polyplex Micelle Based on a Lactosylated ABC Triblock Copolymer as a Targetable and Endosome-Disruptive Nonviral Gene Vector

Motoi Oishi,[†] Kazunori Kataoka,*[,‡,#] and Yukio Nagasaki*[,†]

Tsukuba Research Center for Interdisciplinary Materials Science (TIMS), University of Tsukuba, 1-1-1 Ten-noudai, Tsukuba, Ibaraki 305-8573, Japan, Department of Materials Engineering, Graduate School of Engineering, The University of Tokyo, 7-3-1 Hongo, Bunkyo-ku, Tokyo 113-8656, Japan, and Division of Clinical Biotechnology, Center for Disease Biology and Integrative Medicine, Graduate School of Medicine, The University of Tokyo, 7-3-1 Hongo, Bunkyo-ku, Tokyo 113-0033, Japan. Received December 24, 2005; Revised Manuscript Received February 21, 2006

Nonviral vectors for gene therapy have recently received an increased impetus because of the inherent safety problems of the viral vectors, while their transfection efficiency is generally low compared to the viral vectors. The lack of the ability to escape from the endosomal compartments is believed to be one of the critical barriers to the intracellular delivery of noviral gene vectors. This study was devoted to the design and preparation of a novel ABC triblock copolymer for constructing a pH-responsive and targetable nonviral gene vector. The copolymer, lactosylated poly(ethylene glycol)-*block*-poly(silamine)-*block*-poly[2-(*N,N*-dimethylamino)ethyl methacrylate] (Lac-PEG-PSAO-PAMA), consists of lactosylated poly(ethylene glycol) (A-segment), a pH-responsive polyamine segment (B-segment), and a DNA-condensing polyamine segment (C-segment). The Lac-PEG-PSAO-PAMA spontaneously associated with plasmid DNA (pDNA) to form three-layered polyplex micelles with a PAMA/pDNA polyion complex (PIC) core, an uncomplexed PSAO inner shell, and a lactosylated PEG outer shell, as confirmed by ^{1}H NMR spectroscopy. Under physiological conditions, the Lac-PEG-PSAO-PAMA/pDNA polyplex micelles prepared at an N/P (number of amino groups in the copolymer/number of phosphate groups in pDNA) ratio above 3 were found to be able to condense pDNA, thus adopting a relatively small size (< 150 nm) and an almost neutral surface charge ($\zeta \sim +5$ mV). The micelle underwent a pH-induced size variation (pH = 7.4, 132.6 nm → pH = 4.0, 181.8 nm) presumably due to the conformational changes (globule-rod transition) of the uncomplexed PSAO chain in response to pH, leading to swelling of the free PSAO inner shell at lowered pH while retaining the condensed pDNA in the PAMA/pDNA PIC core. Furthermore, the micelles exhibited a specific cellular uptake into HuH-7 cells (hepatocytes) through asialoglycoprotein (ASGP) receptor-mediated endocytosis and achieved a far more efficient transfection ability of a reporter gene compared to the Lac-PEG-PSAO/pDNA and Lac-PEG-PAMA/pDNA polyplex micelles composed of the diblock copolymers and pDNA. The effect of hydroxychloroquine as an endosomolytic agent on the transfection efficiency was not observed for the Lac-PEG-PSAO-PAMA/pDNA polyplex micelles, whereas the nigericin treatment of the cell as an inhibitor for the endosomal acidification induced a substantial decrease in the transfection efficiency, suggesting that the protonation of the free PSAO inner shell in response to a pH decrease in the endosome might lead to the disruption of the endosome through buffering of the endosomal cavity. Therefore, the polyplex micelle composed of ABC (ligand-PEG/pH-responsive segment/DNA-condensing segment) triblock copolymer would be a promising approach to a targetable and endosome disruptive nonviral gene vector.

INTRODUCTION

Nonviral vectors for gene therapy have recently received increased attention because of the concerns over the safety issues of viral vectors, including immunogenicity, oncogenicity, and potential virus recombination (*1*–*3*). Most of the nonviral vectors developed so far, however, show low transfection efficiency compared to the viral vectors, because the latter have evolved multi-functionality to overcome the critical barrier to efficient gene delivery by directing the specific cellular uptake and enhancing transport to the cytoplasm from the endosomal compartment. Recently, a new class of nonviral gene vectors has been developed based on the supramolecular assembly between plasmid DNA (pDNA) and poly(ethylene glycol) (PEG)-*block*-polyamine copolymers (polyplex micelles) (*4*–*10*). Because of the highly dense PEG shell surrounding the polyion complex (PIC) core, the polyplex micelles exhibited excellent solubility in aqueous media, high tolerability toward nuclease degradation, and minimal interaction with biological components, including proteins and cells, compared to the other conventional polyplex and lipoplex systems. Furthermore, ligand-installed polyplex micelles prepared from lactosylated PEG-*block*-poly[2-(*N,N*-dimethylamino)ethyl methacrylate] copolymer and pDNA showed an increase in the cellular uptake through a receptor-mediated endocytosis process compared to those without lactose (ligand) moieties (*11*). To observe an appreciable effect of the ligand molecules on gene expression, however, the presence of hydroxychloroquine (100 μM) as an endosomolytic agent (*12*, *13*) has so far been required. This indicates that endosomal escape should be the most critical

* To whom correspondence should be addressed. (Y.N.) Phone: +81-29-853-5749. Fax: +81-29-853-5749. E-mail: nagasaki@nagalabo.jp; (K.K.) Phone +81-3-5841-7139. Fax: +81-3-5841-7139. E-mail: kataoka@bmw.t.u-tokyo.ac.jp.

† Tsukuba Research Center for Interdisciplinary Materials Science (TIMS), University of Tsukuba.

‡ Department of Materials Engineering, The University of Tokyo.

Division of Clinical Biotechnology, The University of Tokyo.

10.1021/bc050364m CCC: $33.50
Published on Web 04/15/2006

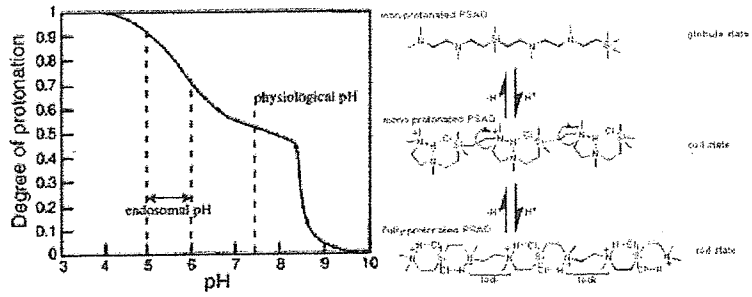

Figure 1. Change in the protonation degree of poly(silamine) (PSAO) with pH accompanying the conformation transition (globule-coil-rod).

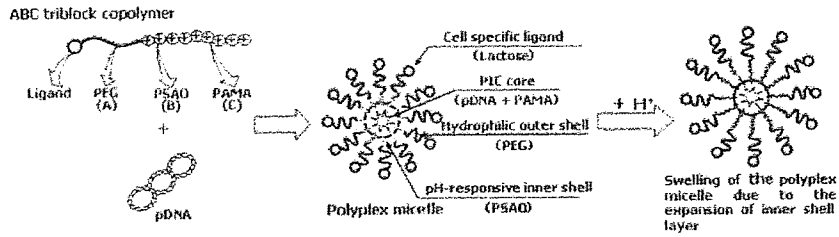

Figure 2. Schematic illustration of the formation of the three-layered polyplex micelle composed of the ABC triblock copolymer and pDNA.

barrier to intracellular gene delivery by polyplex micelles (*14*–*16*). Therefore, approaches are needed to devise polyplex micelles with a function to escape from the endosome where the pH is 1.4–2.4 units lower than the physiological pH of 7.4 (*17*–*20*). In this regard, poly(ethylenimine) (PEI) derivatives are of interest as a pH-responsive polyamine component to accomplish endosomal escape by taking advantage of their substantially lowered value of apparent pK_a (~5.5) ("buffer or proton-sponge effect") (*21*). However, the buffer effect of the PEI segment occurs only when an excess of amino groups with respect to DNA phosphate groups (high N/P ratio) is present in the system, where a considerable amount of the amino groups in PEI is in the free-base form. This fact strongly suggests that free PEI, which is not complexed with pDNA, is likely to play a crucial role in the buffer effect, because amino groups in the PEI/pDNA polyplex generally undergo facilitated protonation due to the zipper effect or the neighboring group effect during the polyion complexation (over-protonation) to decrease the buffering capacity (*22*). Therefore, a strategy is needed to satisfy the prevention of overprotonation of the pH-responsive polyamine segment in the polyplex, as well as the achievement of efficient condensation of pDNA into the PIC core to exert efficient stability. Worth noting in this regard is a concomitant incorporation of the polyamine segment with a high pK_a and one with a low pK_a into a single PEG-based strand, as an ABC triblock copolymer (*23*). A polyamine segment with a high pK_a as the C block preferentially forms a polyion complex with phosphate groups in pDNA (DNA-condensation segment), whereas the pH-responsive polyamine segment (B block) with a comparatively low pK_a, located between the PEG segment (A block) and the pDNA-condensation segment (C block), is expected to retain a substantial fraction of unprotonated amino groups (free-base) even in the polyplex due to the low protonation ability. As a consequence, the polyion complexation between such an ABC triblock copolymer and pDNA may lead to the formation of a three-layered polyplex micelle possessing an unprotonated pH-responsive polyamine segment as an intermediate layer to function as a buffering moiety for facilitated endosomal escape.

We herein synthesized a novel ABC triblock copolymer composed of a targetable and biocompatible polymer segment, a pH-responsive polyamine segment, and a DNA-condensing polyamine segment to form a three-layered polyplex micelle: lactosylated PEG-*block*-poly(silamine) (PSAO) -*block*-poly[2-(*N,N*-dimethylamino)ethyl methacrylate] (PAMA) [Lac-PEG-PSAO-PAMA]. Here, PSAO was selected as the pH-responsive polyamine segment showing two-step protonation (Figure 1, pK_{a1} = 8.6 and pK_{a2} = 5.8) along with a unique conformational transition at the critical pH (*24*–*29*). The unprotonated PSAO is insoluble in water, assuming a globular conformation with high flexibility, whereas fully protonated PSAO is soluble in water, assuming a rodlike conformation with rigid and expanded polymer strands. Such a unique conformational transition (rod-globule transition) can be explained by the rotational hindrance around the polymer chain due to the protonation of the amino groups along with the counteranion binding to the Si atoms (Figure 1). On the other hand, PAMA (pK_a = 7.2) is known to condense pDNA to form a compact structure, the size of which is less than 200 nm under physiological conditions (*8*, *30*, *31*). This fact suggests that polyion complexation between the Lac-PEG-PSAO-PAMA and pDNA may form a targetable and endosome disruptive polyplex micelle with a well-defined three-layered structure (Figure 2).

EXPERIMENTAL SECTION

Materials. 2,2′-Azobisisobutyronitrile (AIBN), dicyclohexylcarbodiimide (DCC), *N*-hydroxysuccinimide (NHS), and nigericin (NR) were purchased from Wako and used without further purification. Asialofetuine (ASF) and hydroxychloroquine sulfate (HCQ) were purchased from Sigma and Acros Organics, respectively. Potassium naphthalene was used as a THF solution, whose concentration was determined by titration. Water was purified using a Milli-Q instrument (Millipore). 2-Propanol and diethyl ether (Et_2O) were used as received without further purification. Lysotraker Red DND-99 was purchased from Molecular Probes. Plasmid DNA (pDNA) encoding firefly luciferase (pGL3-Luc, Promega; 5256 bpa) was amplified using EndoFree Plasmid Maxi or Mega kits (QIAGEN). The DNA concentration was determined by reading the absorbance at 260 nm.

Polymer Analysis. ^{1}H NMR (400 MHz) spectra were obtained in $CDCl_3$, DMSO-d_6, or D_2O (pD = 7.4 and 4.0) with 0.15 M NaCl using a JEOL EX400 spectrometer. Chemical shifts were reported in ppm relative to $CDCl_3$ (δ7.26, ^{1}H), DMSO-d_6 (δ 2.50, ^{1}H), or D_2O buffer (δ 4.76, ^{1}H). Size exclusion chromatography (SEC) was performed using a TOSO

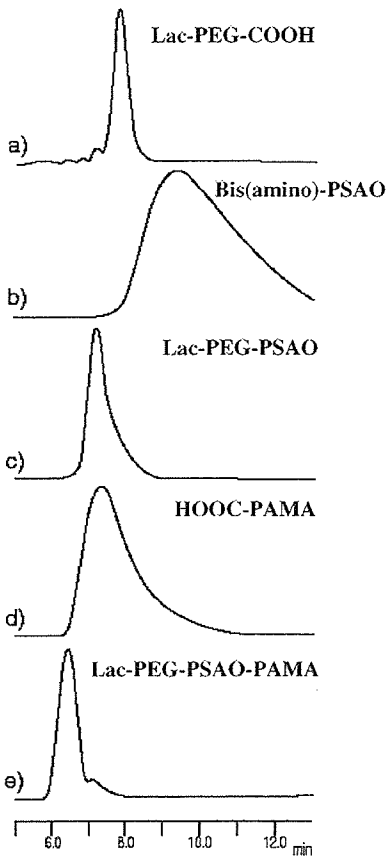

Figure 3. SEC chromatograms of the (a) Lac-PEG-COOH, (b) bis(amino)-PSAO, (c) Lac-PEG-PSAO block copolymer, (d) HOOC-PAMA, and (e) Lac-PEG-PSAO-PAMA triblock copolymer.

HLC-8020 equipped with an internal refractive index (RI) detector (RID-6A) with the combination of TSK G4000$_{HR}$ and G3000$_{HR}$ columns using THF as the eluent.

Synthesis of Lactose-PEG-*block*-PSAO. Bis(amino)-PSAO was synthesized according to our previous report (*24*−*29*). The Lac-PEG-COOH (0.100 g, 16 μmol) and an excess amount of bis(amino)-PSAO (1.244 g 800 μmol, M_n = 1550, DP = 6) were dissolved in $CHCl_3$ (5.0 mL) together with DCC (6.3 mg, 32 μmol) and NHS (2.3 mg, 20 μmol). The reaction mixture was stirred at room temperature for 72 h. To remove the unreacted bis(amino)-PSAO and other chemicals, the reaction mixture was poured into Et_2O (200 mL). The obtained polymer was further purified by reprecipitation into Et_2O (200 mL) and then freeze-dried with benzene to obtain the lactose-PEG-*b*-PSAO (0.102 g, 83% yield). Figures 3c and 4a, respectively, show the SEC chromatogram and ^{1}H NMR spectrum of Lac-PEG-PSAO with assignment. SEC M_n = 7170, M_w/M_n = 1.15 (calcd. M_n = 7850); ^{1}H NMR ($CDCl_3$, in Figure 4a) δ 0.10 (s, 36H, H_k), 0.63−0.79 (m, 24H, H_j), 1.02 (t, J = 7.3 Hz, 36H, H_i), 1.10 (t, J = 7.1 Hz, 3H, H_i''), 1.16 (t, J = 7.1 Hz, 3H, H_i'), 1.77−2.02 (m, 4H, H_d+H_f), 2.42 (t, J = 7.1 Hz, 2H, H_g), 2.47−2.62 (m, 80H, H_h), 2.62−2.73 (m, 2H, H_c), 3.61 (s, 617H, H_a+H_b+H_e)

Synthesis of Lactose-PEG-*block*-PSAO-*block*-PAMA. A PAMA homopolymer bearing a carboxylic acid group at the α-end (HOOC-PAMA) was synthesized via anionic polymerization of 2-(*N*,*N*-dimethylamino)ethyl methacrylate (*32*) using the allyl alcohol/potassium-naphthalene initiator system, followed by the radical addition of 3-mercaptopropionic acid in the presence of AIBN. The Lac-PEG-PSAO (0.051 g, 7.8 μmol) and an excess amount of HOOC-PAMA bearing a carboxylic acid group at the α-end (0.5017 g, 88.5 μmol, M_n = 5670, DP = 35) were dissolved in $CHCl_3$ (5.0 mL) together with DCC (3.2 mg, 16 μmol) and NHS (1.6 mg, 10 μmol). The reaction mixture was stirred at room temperature for 72 h. To remove the unreacted HOOC-PAMA and other chemicals, the polymer was recovered by precipitation into cold 2-propanol (−15 °C, 200 mL) and centrifuged for 45 min at 6000 rpm. Further purification was carried out by dialyzing against distilled, deionized water (cutoff MW 3500) and then freeze-dried to obtain Lac-PEG-PSAO-PAMA (0.0383 g, 37% yield). Figures 3e and 4b, respectively, show the SEC chromatogram and ^{1}H NMR spectrum of Lac-PEG-PSAO-PAMA with assignment. SEC M_n = 10850, M_w/M_n = 1.29 (calcd. M_n = 13450); ^{1}H NMR ($CDCl_3$, in Figure 4b) δ 0.10 (s, 36H, H_d), 0.63−0.79 (m, 24H, H_c), 0.80−1.16 (m, 94H, H_g), 1.02 (t, J = 7.3 Hz, 42H, H_e), 1.16−2.17 (m, 64H, H_f), 2.23 (s, 185H, H_j), 2.37−2.84 (m, 143H, H_b + H_i), 3.61 (s, 617H, H_a), 4.08 (s, 62H, H_h).

Light Scattering Measurements of Polyplex Micelles. To prepare stock solutions, specific amounts of each of the block copolymers (Lac-PEG-PSAO-PAMA, Lac-PEG-PSAO, and Lac-PEG-PAMA) were dissolved in 10 mM Tris-HCl buffer (pH 7.4) or distilled, deionized water, followed by adjustment of the pH to 7.4. Both solutions were filtered through a 0.1-μm filter to remove dust prior to the measurement. For the dynamic light scattering (DLS) measurements as a function of pH, the Lac-PEG-PSAO-PAMA copolymer in distilled water at pH 7.4 including 0.15 M NaCl was mixed with pDNA at an N/P ratio of 3 [N/P = (amino group in the block copolymer)/(phosphate groups in pDNA)] at pH 7.4 to obtain the final concentration of 33.3 μg/mL of pDNA in the solution. The sample solutions were adjusted to the desired pH using small aliquots of 0.1 or 0.01 M HCl, and the DLS was measured at each pH point (pH = 7.0, 6.5, 6.0, 5.5, 5.0, 4.5, and 4.0).

For the DLS measurements of the samples prepared at various N/P ratios, the block copolymer in 10 mM Tris-HCl buffer (pH 7.4) was mixed with pDNA at various N/P ratios (N/P = 1, 2, 3, 4, 5, 7, and 10), followed by the addition of 10 mM Tris-HCl buffer (pH 7.4) including 0.3 M NaCl to adjust the pDNA concentration (33.3 μg/mL) and the ionic strength of the solution to physiological conditions (0.15 M NaCl).

A light-scattering spectrometer (DLS-7000, Photal, Otsuka Electronics) equipped with a 75 mW Ar-laser that produces a vertically polarized incident beam at λ_0 = 488 nm was used in the present study for the DLS measurements.

During the DLS measurements, the autocorrelation function was analyzed using the cumulant method in which

$$g^{(1)}(\tau) = \exp[-\bar{\Gamma}\tau + (\mu_2/2)\tau^2 - (\mu_3/3!)\tau^3 + \cdots] \quad (1)$$

yielding an average characteristic line width of $\bar{\Gamma}$. The z-averaged diffusion coefficient was obtained from the $\bar{\Gamma}$ based on the following equations:

$$\bar{\Gamma} = Dq^2 \quad (2)$$

$$q = (4\pi n/\lambda)\sin(\theta/2) \quad (3)$$

where q is the magnitude of the scattering vector, n is the refractive index of the solvent, and θ is the detection angle. The hydrodynamic radius, d, can then be calculated using the Stokes−Einstein equation:

$$d = k_B T/(6\pi\eta D) \quad (4)$$

where k_B is the Boltzmann constant, T is the absolute temperature, and η is the viscosity of the solvent. Also, the polydispersity index (PDI = μ_2/Γ^2) was derived from eq 1.

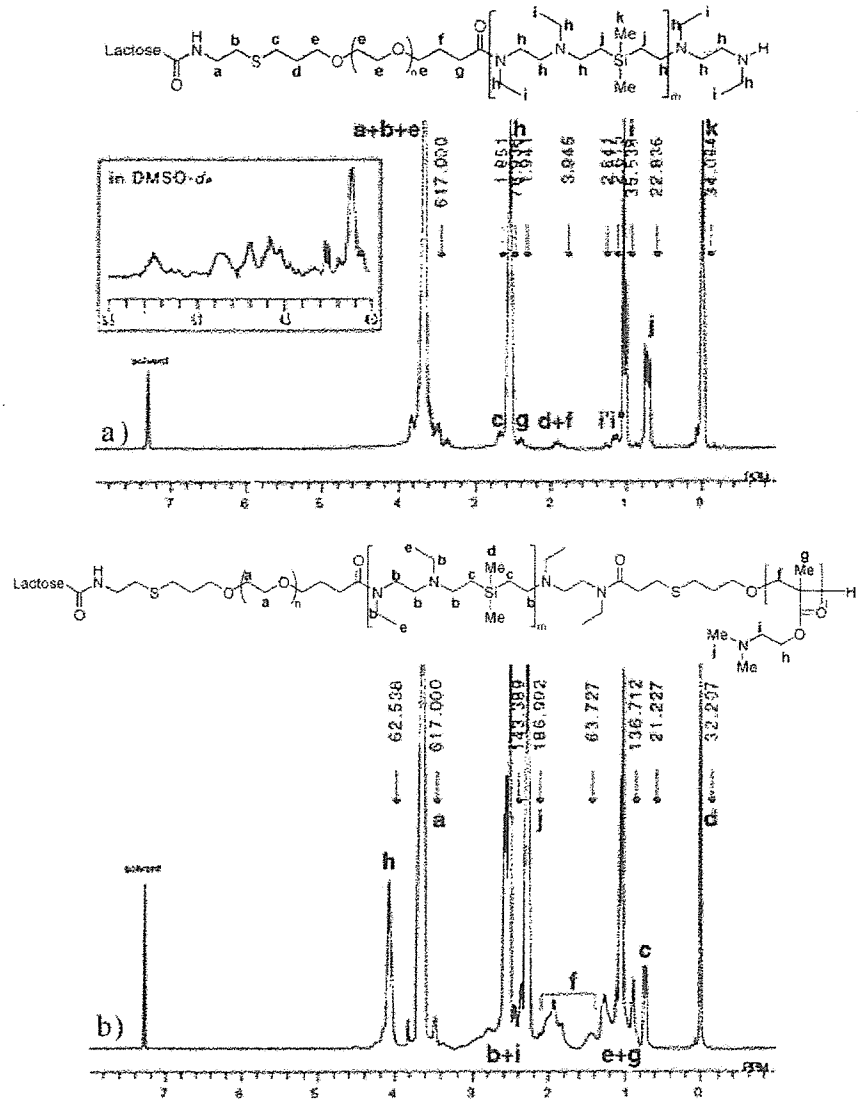

Figure 4. ^{1}H NMR spectra of (a) Lac-PEG-PSAO diblock copolymer and (b) Lac-PEG-PSAO-PAMA triblock copolymer.

Zeta-Potential Measurements. Laser-Doppler electrophoresis measurements of the polyplex micelles were carried out in 10 mM Tris-HCl buffer (pH 7.4) without NaCl (ELS-600, Photal, Otsuka Electronics). From the determined electrophoretic mobility, the zeta-potential (ζ) was calculated according to the Smoluchouski equation as follows:

$$\zeta = 4\pi n\eta\mu u/\epsilon \qquad (5)$$

where η is the viscosity of the solution, u is the electrophoretic mobility, and ϵ is the dielectric constant of the solvent.

Ethidium Bromide Exclusion Assay. The polyplex micelle solutions at various N/P ratios were mixed with ethidium bromide (EtBr) solution, and the final concentration was adjusted to [pDNA] = 20 μg/mL and [EtBr] = 0.4 μg/mL. The fluorescence of the intercalated EtBr was measured on a spectrofluorometer (F-2500, Hitachi) by exciting at 510 nm while monitoring emission at 590 nm.

Agarose Gel Retardation Studies. Aliquots (10 μL) of the above polyplex micelle solutions with various N/P ratios were mixed with 13 μL of running buffer of 3.3 mM Tris-AcOH with 1.0 mM EDTA2Na (pH 7.4) and loaded onto a 0.9 wt % agarose gel (50 V, 2 h). The amount of pDNA was adjusted to 0.3 μg of pDNA/lane. After EtBr (0.5 μg/mL) staining for 1 h, retardation of pDNA was visualized under UV irradiation.

Cell Culture. HuH-7 human cancer cells, derived from a hepatocarcinoma cell line, were obtained from the Cell Resource Center for Biomedical Research, Institute of Development, Aging and Cancer, Tohoku University. The cells were grown in Dulbecco's modified Eagle's medium (DMEM) supplemented with 10% FBS, 100 units/mL penicillin, and 100 μg/mL streptomycin at 37 °C in a humidified 5% CO_2 atmosphere.

Fluorescent Microscopy. Fluorescein isothiocyanate (FITC)-labeled pDNA was prepared using a Label IT nucleic acid labeling kit (Panvera). HuH-7 cells were seeded at a density of 5×10^5 cells/dish in a 35-mm glass bottom dish (Iwaki, Japan) and kept overnight at 37 °C in 5% CO_2 atmosphere. The Lac-PEG-PSAO-PAMA/pDNA polyplex micelles (N/P = 3) were added at a pDNA concentration of 30 μg/mL and incubated at 37 °C in 5% CO_2 atmosphere in the presence or absence of ASF (10 mg/mL) for 60 min. The cells were washed with phosphate buffered saline (PBS) three times and imaged directly in the cell culture medium using an Olympus IX70 with an appropriate filter.

Confocal Fluorescent Microscopy. HuH-7 cells were seeded at a density of 5×10^5 cells/dish in a 35-mm glass bottom dish

Scheme 1. Synthetic Route of Lac-PEG-PSAO-PAMA Block Copolymer

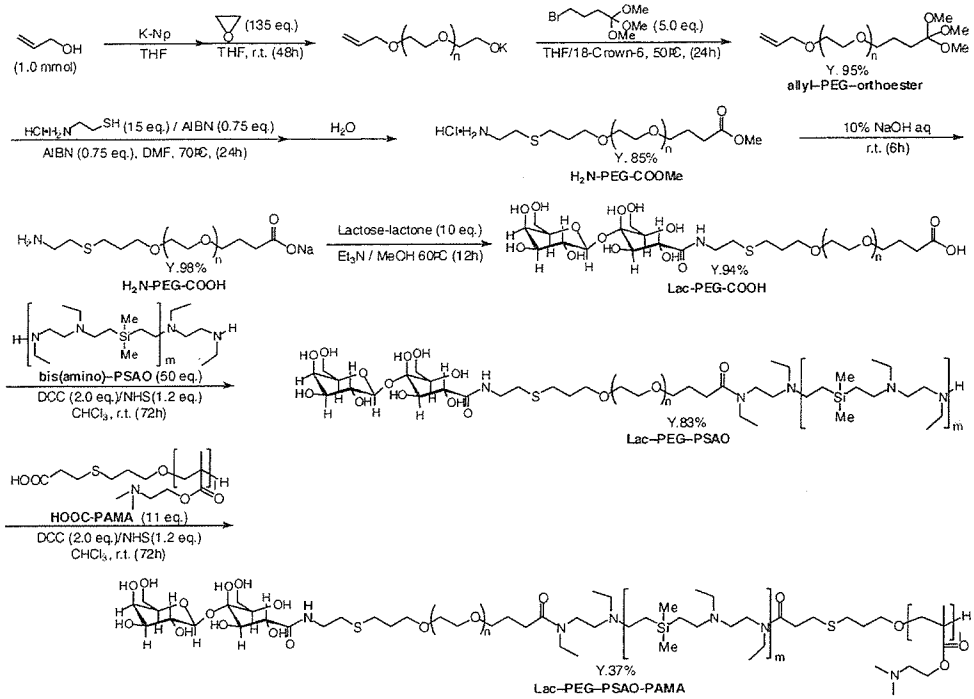

(Iwaki, Japan) and kept overnight at 37 °C in 5% CO_2 atmosphere. The Lac-PEG-PSAO-PAMA/pDNA and the Lac-PEG-PAMA/pDNA polyplex micelles (N/P = 3) containing FITC-labeled pDNA were added at a pDNA concentration of 30 μg/mL and incubated at 37 °C in 5% CO_2 atmosphere in the presence of Lysotraker Red DND-99 (50 nM) for 30 and 120 min. The cells were washed with PBS three times and imaged directly in the cell culture medium using an Olympus IX81 equipped with a confocal IX2-DSU system and an appropriate filter.

Transfection to HuH-7 Cells. HuH-7 cells were plated in a 24-well plate (5×10^4 cells/well) to reach about 50% confluence after 24 h at transfection, and the medium was then changed to fresh DMEM with 10% FBS (225 μL/well). For each well, the polyplex micelles or B-PEI/pDNA polyplexes at various N/P ratios (25 μL/well) were added with a pDNA concentration of 30 μg/mL. After 24 h incubation, the transfection medium was changed to fresh DMEM with 10% FBS, and the cells were further incubated for 24 h. For the preincubation study with serum, a medium containing 20% FBS was added to the solution of the polyplex micelles or B-PEI/pDNA polyplexes and incubated at 37 °C for 6 h prior to the transfection study. The cells were lysed, and the luciferase activity of the lysate was monitored with the a Luciferase Assay kit (Promega) and ARVOSX-1 (PerkinElmer). The results were expressed as light units per milligram of cell protein determined by a micro BCA assay kit (Pierce).

RESULTS AND DISCUSSION

Synthesis of Lactosylated Poly(ethylene glycol)-*block*-poly(silamine)-*block*-poly[2-(*N,N*-dimethlyamino)ethyl methacrylate] Triblock Copolymer. A synthetic route to lactosylated poly(ethylene glycol)-*block*-poly(silamine)-*block*-poy[2-(*N,N*-dimethlyamino)ethyl methacrylate] (Lac-PEG-PSAO-PAMA) triblock copolymer is shown in Scheme 1. A heterobifunctional PEG bearing an allyl group at the α-end and an ortho ester group at the ω-end (allyl-PEG-ortho ester) was synthesized via the anionic ring-opening polymerization of ethylene oxide using the allyl alcohol /potassium-naphthalene initiator system, followed by termination with trimethyl 4-bromoorthobutyrate in the presence of 18-Crown-6. The radical addition of 2-aminoethanethiol hydrochloride to the allyl-PEG-ortho ester quantitatively afforded an amine-PEG-methoxycarbonyl (H_2N-PEG-COOMe). Conversion of the ortho ester group into a methoxycarbonyl group (COOMe) occurred due to the hydrolysis of the ortho ester group during the purification (dialysis) process. The H_2N-PEG-COOMe was then converted into an amine-PEG-carboxylic acid (H_2N-PEG-COOH) by hydrolysis with 10% NaOHaq. The SEC (data not shown), ^1H NMR, and MALDI-TOF MS analyses (see Supporting Information) revealed that the determined molecular weight of the H_2N-PEG-COOH (SEC: $M_n = 6200$, $M_w/M_n = 1.04$, TOF-MS: $M_n = 6190$, $M_w/M_n = 1.03$) agrees well with the calculated value (calcd. $M_n = 6130$), and an amino group and carboxylic acid group were quantitatively introduced into the α-end and ω-end of PEG, respectively, to confirm the successful synthesis of allyl-PEG-ortho ester and H_2N-PEG-COOMe. The introduction of a lactose group to the amine end of H_2N-PEG-COOH was performed by reaction with an excess amount of lactose-lactone (*33*). In the ^1H NMR spectrum of Lac-PEG-COOH, the degree of lactose functionality was determined to be 72% (see Supporting Information).

To obtain the lactosylated PEG-PSAO block copolymer, bis(amino)-PSAO ($M_n = 1550$, the degree of polymerization (DP) = 6) was prepared as reported previously by the anionic polyaddition of dimethyldivinylsilane with *N,N'*-diethylethylenediamine in the presence of a catalytic amount of *n*-BuLi in THF at 60 °C (*24*−*29*). The conjugation of the Lac-PEG-COOH with bis(amino)-PSAO was performed by activating the terminal carboxylic acid of Lac-PEG-COOH using dicyclohexylcarbodiimide (DCC) and *N*-hydroxysuccinimide (NHS). A large excess (50 equiv) of the bis(amino)-PSAO was used to suppress the formation of triblock coplymer viz., Lac-PEG-PSAO-PEG-Lac. After the conjugation reaction, unconjugated bis(amino)-PSAO and other chemicals were removed by precipitation into Et_2O. Figures 3c and 4a, respectively, show the SEC chromatogram and ^1H NMR spectrum of the Lac-PEG-PSAO block

Table 1. Diameter (d), PDI (μ_2/Γ^2), and Zeta-Potential (ζ) of the Lac-PEG-PSAO-PAMA/pDNA, Lac-PEG-PAMA/pDNA, and Lac-PEG-PSAO/pDNA Polyplex Micelles Prepared at Various N/P Ratios

N/P ratio	Lac-PEG-PSAO−PAM A polyplex micelles		Lac-PEG-PAMA polyplex micelles		Lac-PEG-PSAO polyplex micelles	
	DLS[a] d (nm) /PDI (μ_2/Γ^2)	zeta-potential[b] (mV)	DLS[a] d (nm)/ PDI (μ_2/Γ^2)	zeta-potential[b] (mV)	DLS[a] d (nm)/ PDI (μ_2/Γ^2)	zeta-potential[b] (mV)
1	200.3/0.23	−4.3	196.5/0.24	−3.8	178.9/0.24	−5.8
2	175.4/0.23	+3.6	180.9/0.22	+3.8	166.6/0.20	−1.2
3	149.1/0.14	+4.7	147.0/0.14	+4.6	157.0/0.17	+0.6
4	147.2/0.17	+5.3	141.5/0.17	+4.8	163.4/0.22	+1.7
5	147.4/0.13	+5.1	140.0/0.19	+4.7	140.1/0.12	+2.3
7	146.8/0.18	+5.5	141.6/0.14	+5.0	144.7/0.19	+2.5
10	145.5/0.18	+5.4	136.1/0.12	+4.8	145.2/0.17	+2.4

[a] Conditions for DLS measurements: detection angle, 90°; solvent, 10 mM Tris-HCl, pH 7.4, including 0.15 M NaCl; temperature, 37 °C. [b] Conditions for zeta-potential measurements: solvent, 10 mM Tris-HCl, pH 7.4; temperature, 25 °C.

copolymer with assignments. As seen in the SEC chromatograms (Figure 3), Lac-PEG-PSAO (Figure 3c) gave a unimodal peak at a high molecular weight position (i.e., shorter elution time) compared to the Lac-PEG-COOH (M_n = 6300, M_w/M_n = 1.05, Figure 3a) and bis(amino)-PSAO (M_n = 1550, M_w/M_n = 2.01, Figure 3b). Note that the unreacted Lac-PEG-COOH and bis(amino)-PSAO were not observed in the SEC chromatogram (Figure 3c) of the Lac-PEG-PSAO (obsd. M_n = 7150, M_w/M_n = 1.15, calcd. M_n = 7850). In the ^{1}H NMR spectrum (Figure 4a), the peaks corresponding to both of the PEG and PSAO segments were clearly observed, consistent with the formation of a diblock copolymer. Note that the peaks corresponding to the terminal lactose moiety were also observed at δ 4.0−5.3 ppm in the ^{1}H NMR spectrum in DMSO-d_6. From the integral ratio between the PEG-backbone protons (3.7 ppm -OCH_2CH_2-) and the methyl protons of PSAO segment (0.1 ppm, $SiMe_2$), the DP of the PSAO segment in the block copolymer was calculated to be 5.67, which is in good accordance with that of the starting bis(amino)-PSAO (DP = 6).

To obtain the Lac-PEG-PSAO-PAMA triblock copolymer, the conjugation of the Lac-PEG-PSAO diblock copolymer and HOOC-PAMA was performed in a manner similar to the conjugation of Lac-PEG-COOH and bis(amino)-PSAO. After the conjugation reaction, unconjugated HOOC-PAMA and other chemicals were removed by precipitation into cold 2-propanol, followed by centrifugation. Figures 3c and 4b, respectively, show the SEC chromatogram and ^{1}H NMR spectrum of the Lac-PEG-PSAO-PAMA triblock copolymer with assignments. The Lac-PEG-PSAO-PAMA (Figure 3c, M_n = 10850, M_w/M_n = 1.29, calcd. M_n = 13450) had a shorter elution time compared to the Lac-PEG-PSAO (M_n = 7170, M_w/M_n = 1.15, Figure 3c) and HOOC-PAMA (M_n = 5670, M_w/M_n = 1.50, DP = 35, Figure 3d), indicating an increased molecular weight due to the formation of the triblock polymer. Nevertheless, a slight portion of unreacted Lac-PEG-PSAO and/or HOOC-PAMA seems to still remain (about 10%) in the sample as indicated by the small accompanying peak appearing after the main fraction (Figure 3c). In thethe ^{1}H NMR spectrum (Figure 4b), the peaks corresponding to the PEG, PSAO, and PAMA segments were clearly observed, suggesting the formation of a triblock copolymer. From the integral ratio between the PEG-backbone protons (3.7 ppm -OCH_2CH_2-) and methylene protons of the PAMA segment (4.08 ppm, -COOCH_2CH_2N(CH_3)$_2$), the DP of the PAMA segment was calculated to be 31.3 (DP of starting PAMA = 35). This result indicates that the purity of the triblock copolymer was 89%.

Furthermore, Lac-PEG-PSAO (M_{nPEG} = 6300, DP_{PSAO} = 6, number of amino groups = 12) and Lac-PEG-PAMA (M_{nPEG} = 6300, DP_{PAMA} = 55, number of amino groups = 55) diblock copolymers were prepared in a similar manner as the controls for the Lac-PEG-PSAO-PAMA (M_{nPEG} = 6300, DP_{PSAO} = 6, DP_{PAMA} = 35, total number of amino groups = 47).

Physicochemical Characterization of Polyplex Micelles. The obtained triblock (Lac-PEG-PSAO-PAMA) and diblock (Lac-PEG-PAMA and Lac-PEG-PSAO) copolymers form polyplex micelles through the mixing with pDNA based on electrostatic interaction. The size and surface charge of the polyplex micelles (Lac-PEG-PSAO-PAMA/pDNA, Lac-PEG-PAMA/pDNA, and Lac-PEG-PSAO/pDNA) was respectively evaluated by dynamic light scattering (DLS) and Laser-Doppler electrophoresis measurements at various N/P ratios, as summarized in Table 1. In the DLS measurements, the diameter (d) and polydipersity index (PDI; μ_2/Γ^2) of all the polyplex micelles decreased with increasing N/P ratios and reached plateau values of ca. 150 nm and 0.2, respectively, at an N/P ratio higher than 5. Concomitantly, as the N/P ratios increased, the zeta-potential (ζ) of all the polyplex micelles gradually shifted from a negative value (ζ < 0) to a positive value (ζ > 0). Nevertheless, the zeta-potential of all the polyplex micelles retained only a slightly positive value (ζ = +5 mV) even when the N/P ratio was increased to 10, suggesting the formation of a PEG corona surrounding the PIC core. These phenomena are consistent with the DNA condensation (coil-globule transition) upon complexation with the polycation segment in the block copolymers (*5*, *9*, *10*). It should also be noted that the N/P ratio to induce complete DNA condensation substantially shifted to a higher value from a stoichiometric mixing ratio (N/P = 1). A similar tendency was observed for the polyplex micelle from the PEG-PAMA block copolymer and pDNA (*4*).

To further clarify the behavior of DNA condensation, the quenching of the fluorescence intensity of the DNA intercalating dye, EtBr, was observed under physiological conditions for all of the polyplex micelles. Note that cationic EtBr is excluded from the DNA minor groove with the progress of the charge neutralization and the subsequent condensation of DNA due to the interaction with polycations, and therefore, this characteristic of EtBr is frequently utilized to estimate the degree of DNA condensation through complexation with a polycation. The profiles are shown in Figure 5a. In line with a trend in the hydrodynamic diameter and zeta-potential variations as shown in Table 1, the fluorescence intensity of EtBr decreased with increasing N/P ratios for all of the polyplex micelles, and the quenching of the fluorescence still continued even in the region of N/P > 1, suggesting that DNA condensation was not completely finished at the stoichiometric mixing ratio (N/P = 1) and that a nonstoichiometric complex may form in the range of N/P > 1. It should be noted that the amino groups of both PAMA and PSAO segments are incompletely protonated at physiological pH (= 7.4) because of their relatively lowered pKa values (PAMA: pK_a = 7.2, and PSAO: pK_{a1} = 8.6, pK_{a2} = 5.8). This may be a reason for the shift of the DNA-condensation point from a stoichiometric mixing ratio (N/P = 1). It should also be noted that a 35% decrease in fluorescence intensity compared to the initial value was observed for Lac-PEG-PSAO, whereas a decrease is more significant (50~55%)

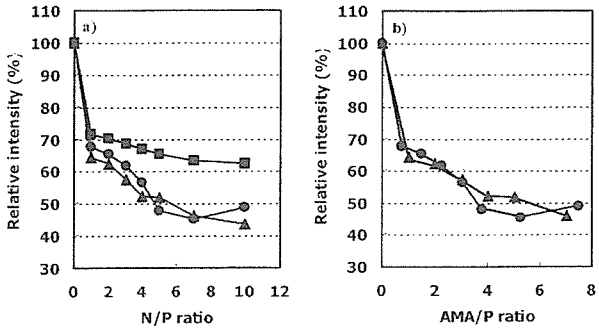

Figure 5. Ethidium bromide (EtBr) exclusion assay for the Lac-PEG-PSAO-PAMA/pDNA (circle), Lac-PEG-PAMA/pDNA (triangle), and Lac-PEG-PSAO/pDNA (square) systems. (a) Change in relative fluorescence intensity with the N/P ratio. (b) Change in relative fluorescence intensity with the AMA/P unit ratio ([amino groups in the PAMA segment]/[phosphate group in the pDNA]) (solvent, 10 mM Tris-HCl buffer including 0.15 M NaCl (pH 7.4); temperature, 37 °C).

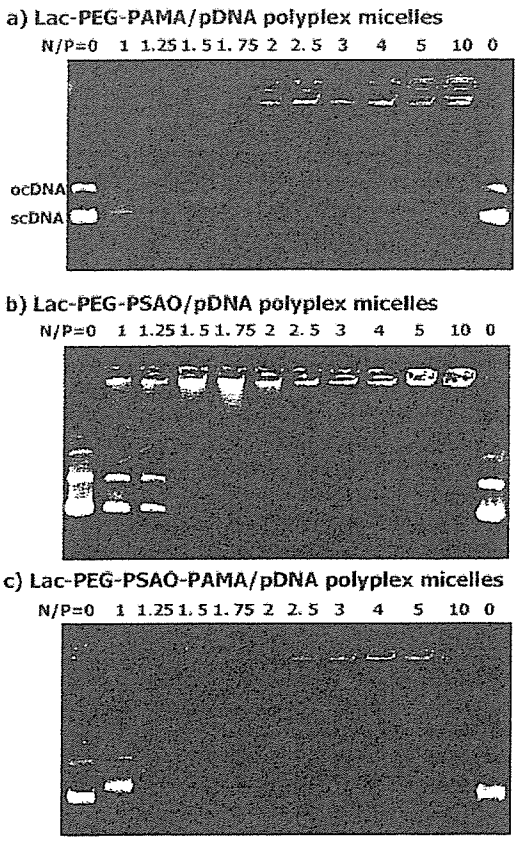

Figure 6. Agarose gel electrophoresis of the (a) Lac-PEG-PAMA/pDNA, (b) Lac-PEG-PSAO/pDNA, and (c) Lac-PEG-PSAO-PAMA/pDNA polyplex micelles prepared at various N/P ratios.

for Lac-PEG-PAMA and Lac-PEG-PSAO-PAMA, and their fluorescence intensities of Lac-PEG-PSAO-PAMA were almost identical when the N/P ratio was converted to the AMA/P ([amino groups in the PAMA segment]/[phosphate group in the pDNA]) unit ratio (Figure 5b), suggesting that the PAMA segment may preferentially take part in the complexation with DNA in the Lac-PEG-PSAO-PAMA/pDNA system, bearing the PSAO segment in the free form.

To evaluate the stability of the polyplex micelle, an agarose gel retardation assay at various N/P ratios was carried out. As shown in Figure 6, two topologically different forms of pDNA, i.e., supercoiled (scDNA) and open circular (ocDNA), were clearly observed in the absence of the block copolymer (at N/P = 0). In the cases of Lac-PEG-PSAO-PAMA/pDNA and Lac-PEG-PAMA/pDNA polyplex micelles, pDNA migration was completely retarded at an N/P ratio ≥ 1.5 (Figure 6a,c). Alternatively, a higher N/P ratio (≥ 3) was required for the complete retardation of pDNA for Lac-PEG-PSAO/pDNA polyplex micelles (Figure 6b). Presumably, excess cationic component may be needed for the Lac-PEG-PSAO block copolymer with a shorter cationic segment to induce effective DNA stabilization.

The polyplex micelle from Lac-PEG-PSAO-PAMA and pDNA was characterized by ^{1}H NMR spectroscopy in D_2O containing 0.15 M NaCl at pD = 7.4. Figure 7f shows the ^{1}H NMR spectrum of the polyplex micelle prepared at N/P = 3, where the residual molar ratio of the protonated PAMA segment in the block copolymer, calculated from the pK_a value, to the phosphate groups in pDNA is estimated to be unity at physiological pH (= 7.4). Note that the DNA condensation process was almost completed at N/P = 3, as shown in Table 1. Obviously, the peaks from the PAMA segment, which were clearly observed in the spectrum of the free polymers (Figure 7c), nearly disappeared upon complexation with pDNA (Figure 7f), whereas the peaks from the PSAO segment were still clearly observed in the spectrum. The selective disappearance of PAMA peaks upon complexation strongly suggests that the PAMA segment predominantly forms a PIC with pDNA to cause significant peak broadening. On the other hand, observation of the peaks from the PSAO segment even in the spectrum of the polyplex micelle suggests the presence of the uncomplexed PSAO fraction. Eventually, these results are consistent with the formation of the three-layered structure of the polyplex micelle with a PAMA/pDNA PIC core, a free PSAO inner shell, and a lactosylated PEG outer shell, as illustrated in Figure 2. In sharp contrast to the Lac-PEG PSAO-PAMA/pDNA system, peaks corresponding to polyamine segments (PAMA and PSAO) completely disappeared in the NMR spectra of the polyplex micelles from diblock copolymers (Lac-PEG-PAMA/pDNA (Figure 7d) and Lac-PEG-PSAO/pDNA (Figure 7e)) due to the limited molecular motion in the complex form.

pH Response of the Polyplex Micelles. To estimate the effect of the environmental pH on the hydrodynamic diameter of the polyplex micelles, the Lac-PEG-PSAO-PAMA/pDNA, Lac-PEG-PSAO/pDNA, and Lac-PEG-PAMA/pDNA polyplex micelles were prepared in 0.15 M NaClaq (pH 7.4) at N/P = 3. By decreasing the pH from 7.4 to 4.0, the diameter (d) of the Lac-PEG-PSAO-PAMA/pDNA and Lac-PEG-PSAO/pDNA polyplex micelles proportionally increases with a unimodal distribution ($\mu_2/\Gamma^2 < 0.25$), reaching a 2.7-times larger hydrodynamic volume at pH 4.0 compared to that at pH 7.4, as shown in Figure 8. On the contrary, there was negligible change in the hydrodynamic diameter of the Lac-PEG-PAMA/pDNA polyplex micelle with decreasing pH from 7.4 to 4.0. This pH-induced size variation observed for the system containing the PSAO segment is most likely to be related to the conformational changes in the PSAO chain due to progressive protonation with decreasing pH. In the ^{1}H NMR spectrum of the Lac-PEG-PAMA/pDNA polyplex micelle (N/P = 3) at pD = 4.0, the peaks from the PAMA segment almost disappeared, indicating that pDNA was still condensed even at pD = 4.0 by the PAMA segment (see Supporting Information). Furthermore, the ^{1}H NMR spectrum of the Lac-PEG-PSAO-PAMA/pDNA polyplex micelle at pD = 4.0 shows only the peaks assigned to the PSAO segment along with the PEG segment, suggesting the three-layered structure even at pD = 4.0 (see Supporting Information). This result supports the plausible scheme that the globule-to-rod conformational changes in the uncomplexed PSAO segment in the three-layered Lac-PEG-PSAO-PAMA/pDNA polyplex

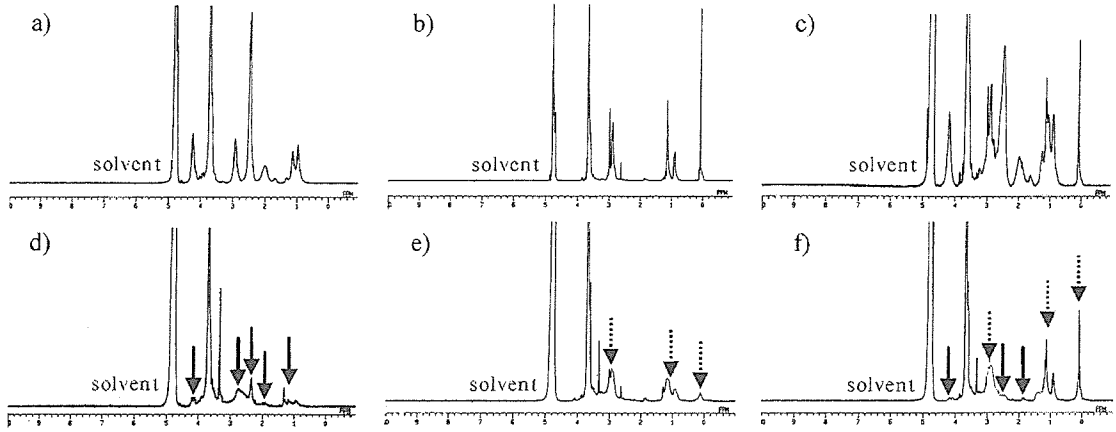

Figure 7. ^{1}H NMR spectra of (a) the Lac-PEG-PAMA block copolymer at pD = 7.4, (b) the Lac-PEG-PSAO block copolymer at pD = 7.4, (c) Lac-PEG-PSAO-PAMA triblock copolymer at pD = 7.4, (d) the Lac-PEG-PAMA/pDNA polyplex micelle at pD = 7.4, (e) the Lac-PEG-PSAO/pDNA polyplex micelle at pD = 7.4, and (f) the Lac-PEG-PSAO-PAMA/pDNA polyplex micelle at pD = 7.4 in D_2O containing 0.15 M NaCl at 37 °C. The solid and dotted arrows indicate the peaks corresponding to the PAMA segment and PSAO segment, respectively.

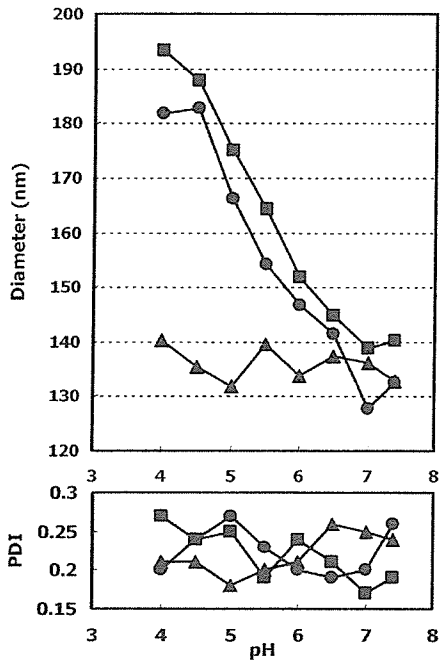

Figure 8. pH vs diameter (d) and PDI (μ_2/Γ^2) of the Lac-PEG-PSAO-PAMA/pDNA (circle), Lac-PEG-PAMA/pDNA (triangle), and Lac-PEG-PSAO/pDNA (square) polyplex micelles at N/P = 3 (angle, 90°; solvent, distilled water including 0.15 M NaCl; temperature, 37 °C).

micelle may induce the selective expansion of the PSAO inner shell while retaining the condensed pDNA in the PAMA/pDNA PIC core, leading to the remarkable pH-induced size variation. However, the observed size variation is clearly too large compared with the calculated PSAO length as the fully stretched chains for coil-state (pH 7.4) and rod-state (pH 4.0), indicating that the expansion of the PSAO inner shell is not sufficient to account for the size variation of the micelles. Although other possible factors probably exist, we believe that the expansion of the PSAO inner shell is one of the factor for the size variation of the micelles. On the other hand, the peaks from the PSAO segment clearly appeared in the ^{1}H NMR spectrum of the Lac-PEG-PSAO/pDNA polyplex micelle at pD = 4.0, suggesting that the conformational changes (globule-rod transition) of the complexed PSAO segment in the Lac-PEG-PSAO/pDNA polyplex micelle presumably leads to the formation of a loose PIC core (see Supporting Information). Apparently, the high rigidity of the protonated PSAO chain in the lower pH region should be unfavorable for triggering the DNA condensation upon complexation. As a consequence, a loose complex may form between pDNA and the PSAO segment without condensation in the lower pH region, showing an appreciable size increase.

Evaluation of the Biological Efficacy of the Polyplex Micelles. The cytotoxicity of the Lac-PEG-PSAO-PAMA, Lac-PEG-PAMA, and Lac-PEG-PSAO block copolymers against HuH-7 cells (hepatocytes) was studied using an MTT assay (see: Supporting Information). The viability of cells treated with the Lac-PEG-PSAO block copolymer was less than 20% at a polymer concentration of 100 μg/mL (IC_{50} < 30 μg/mL). In contrast, cells incubated with Lac-PEG-PSAO-PAMA or Lac-PEG-PAMA retained 65~70% viability relative to controls even at concentrations up to 100 μg/mL. This result indicates that the inclusion of PSAO segment into the Lac-PEG-PSAO-PAMA triblock copolymer seems to substantially reduce its inherent cytotoxicity.

To examine whether the lactose moiety (galactose terminal) on the surface of Lac-PEG-PSAO-PAMA/pDNA polyplex micelle is recognized by the asialoglycoprotein (ASGP) receptors existing on the HuH-7 cells (*34*, *35*), the cellular association and internalization of the polyplex micelle (N/P = 3) with fluorescein isothiocyanate (FITC)-labeled pDNA were visualized under a fluorescence microscope at 60 min of incubation in the presence and absence of asialofetuine (ASF). Note that the ASF is known to function as a competitive inhibitor for the ASGP receptor-mediated endocytosis (*36*). The cellular association and internalization of the Lac-PEG-PSAO-PAMA/pDNA polyplex micelle to HuH-7 cells in the absence of ASF were clearly observed as shown in Figure 9b,d. On the contrary, substantially reduced cellular association and internalization of the micelles were observed in the presence of ASF as shown in Figure 9a,c. This result indicates that the cellular association and internalization of the Lac-PEG-PSAO-PAMA/pDNA polyplex micelle occur mainly through the ASGP receptor-mediated process, which is inhibited in the presence of ASF (*37*).

To estimate the transfection ability of the Lac-PEG-PSAO-PAMA/pDNA, Lac-PEG-PAMA/pDNA, and Lac-PEG-PSAO/pDNA polyplex micelles with various N/P ratios, a transfection study using HuH-7 cells was carried out in the presence of 10% FBS. A pGL-3 control plasmid DNA encoding firefly luciferase was used as a reporter gene. In addition, the B-PEI/pDNA polyplex was used as a control vector at the optimal N/P ratio of 10 to show the highest transfection efficacy. As shown in Figure 10, the transfection efficiency of the Lac-PEG-PSAO-

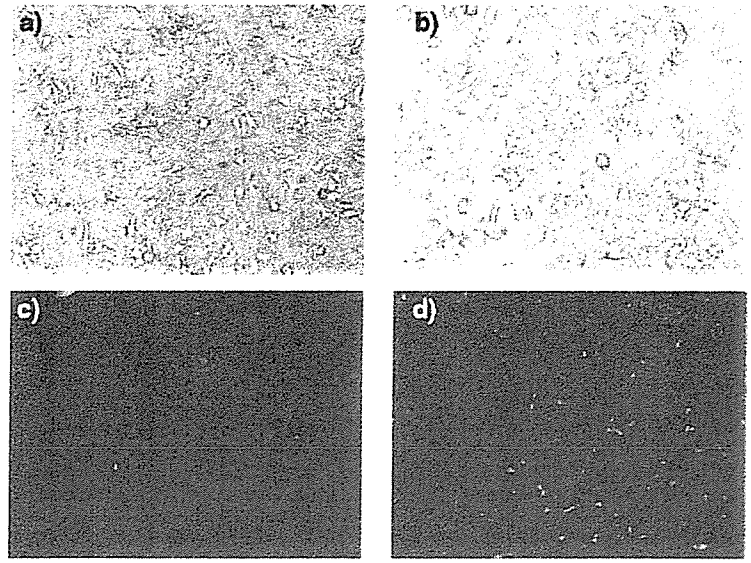

Figure 9. Association and internalization to HuH-7 cells of the Lac-PEG-PSAO-PAMA/pDNA polyplex micelles prepared at N/P = 3 after 60 min incubation. (a) ASF (+) (phase-contrast image), (b) ASF (−) (phase-contrast image), (c) ASF (+) (fluorescent image), and (d) ASF (−) (fluorescent image).

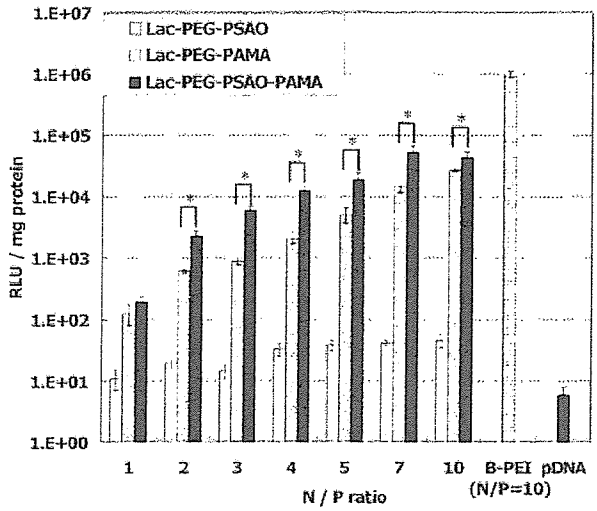

Figure 10. Transfection efficiency to HuH-7 cells of the Lac-PEG-PSAO-PAMA/pDNA, Lac-PEG-PAMA/pDNA, and Lac-PEG-PSAO/pDNA polyplex micelles prepared at various N/P ratios with a fixed pDNA amount. The plotted data are the average of triplicate experiments ± SD ($P^* < 0.05$).

PAMA/pDNA and Lac-PEG-PAMA/pDNA polyplex micelles was substantially improved with an increasing N/P ratio. In particular, 1 order of magnitude increase in transfection efficiency was achieved by increasing the N/P ratio from 1 to 2 ($P < 0.05$), corresponding to the formation of a stable polyplex structure judging from the agarose gel retardation assay, seen in Figure 6. Alternatively, the Lac-PEG-PSAO/pDNA polyplex micelles exhibited only limited transfection efficiency, presumably due to the low DNA condensing capacity of the PSAO chain as indicated from the results of the EtBr exclusion assay shown in Figure 5. Thus, polyplex micelles formed from Lac-PEG-PSAO may not be stable enough to be tolerated in the culture medium containing a substantial amount of serum proteins. Of interest, the transfection efficiency of the Lac-PEG-PSAO-PAMA/pDNA polyplex micelles always revealed a higher transfection efficiency than the Lac-PEG-PAMA/pDNA polyplex micelles in the range of N/P ratios between 2 and 10 ($P < 0.05$).

To determine whether the difference in the transfection efficiency between the Lac-PEG-PSAO-PAMA/pDNA and Lac-PEG-PAMA/pDNA polyplex micelles is related to the endosomal escape function, confocal microscope experiments were performed on the HuH-7 cells treated with the polyplex micelles containing FITC-labeled pDNA. Cells were co-incubated with LysoTracker Red DND-99 probe, which specifically stains acidic organelles such as endosomes and lysosomes. Thus, the colocalization of the polyplex micelles and the LysoTracker Red probe in an acidic compartment (endosome and lysosome) should be detected as yellow (or orange) fluorescence due to the merging of green and red colors. In the case of the Lac-PEG-PAMA/pDNA polyplex micelles (Figure 11a,b), the yellow and red fluorescences were observed without isolated green fluorescence even after a 120-min incubation, indicating that the polyplex micelles localized in the endosomes and/or lysosomes with the LysoTracker Red probe. The Lac-PEG-PSAO-PAMA/pDNA polyplex micelles localized in the endosomes and/or the lysosomes with the LysoTracker Red probe after a 30 min incubation (Figure 11c), as suggested by the partially yellow fluorescence. At 120 min of incubation, diffused green fluorescence was observed in the cytoplasm (Figure 11d), indicating that the Lac-PEG-PSAO-PAMA/pDNA polyplex micelles gradually escaped from the endosomes and/or lysomes into the cytoplasm in a time-dependent manner. These results suggest that both the PAMA segment as a DNA-condensing polycation and the PSAO segment as the buffering moiety may synergistically contribute to enhance the transfection efficiency of the Lac-PEG-PSAO-PAMA/pDNA polyplex micelles. Although the Lac-PEG-PSAO-PAMA/pDNA polyplex micelles showed 1 order of magnitude lower transfection efficiency than the B-PEI/pDNA polyplex at N/P = 10 ($P < 0.05$), this value may still be appreciable considering that the polyplexe micelles have hydrophilic and neutral PEG palisades on their surface to shield the cationic character.

To verify that the improved transfection ability of the Lac-PEG-PSAO-PAMA/pDNA polyplex micelles is a result of the facilitated endosomal escape function as well as the enhanced cellular uptake through ASGP-mediated endocytosis, the transfection study at N/P = 3, 5, and 10 was carried out in the presence or the absence of hydroxychloroquine (HCQ) as an endosomolytic agent, nigericin (NR) (*38*) as an inhibitor of the

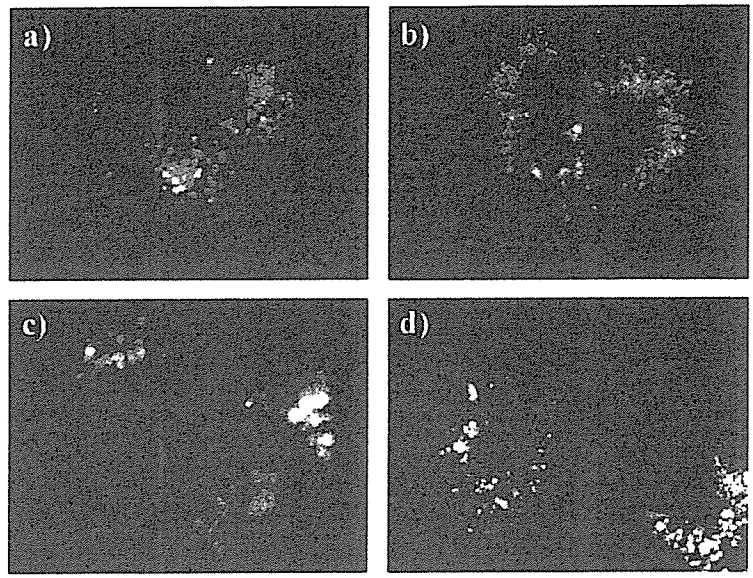

Figure 11. Confocal fluorescent microscope images of the HuH-7 cells in the presence of Lysotracker Red DND-99 and polyplex micelles prepared at N/P = 3 with FITC-labeled pDNA. (a) Lac-PEG-PAMA/pDNA polyplex micelles (incubation time: 30 min), (b) Lac-PEG-PAMA/pDNA polyplex micelles (incubation time: 120 min), (c) Lac-PEG-PSAO-PAMA/pDNA polyplex micelles, (incubation time: 30 min), (d) Lac-PEG-PSAO-PAMA/pDNA polyplex micelles (incubation time: 120 min). These images are the typical image of triplicate experiments.

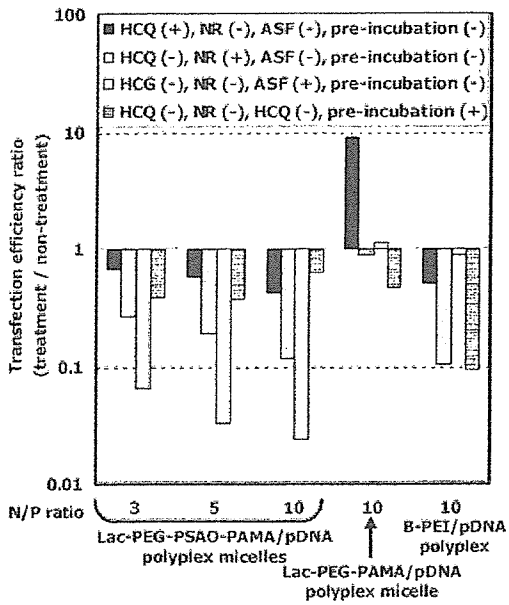

Figure 12. Effect of the HCQ (100 μM), NR (5 μM), ASF (4 mg/mL), and 20% serum preincubation on the transfection efficiency to HuH-7 cells of the Lac-PEG-PSAO-PAMA/pDNA polyplex micelle, Lac-PEG-PAMA/pDNA polyplex micelle, and B-PEI/pDNA polyplex as a function of N/P ratios at a fixed pDNA amount. Transfection efficiency ratio is described as [value of RLU/mg of protein treated with additive (HCQ, NR, and ASF)]/[value of RLU/mg of protein in Figure 11]. The plotted data are the average of triplicate experiments ± SD.

endosomal acidification, and ASF as an inhibitor of the ASGP-mediated endocytosis. As shown in Figure 12, HCQ treatment (100 μM) had no contribution in increasing the transfection efficiency for the Lac-PEG-PSAO-PAMA/pDNA polyplex micelles and the B-PEI/pDNA polyplex compared with the Lac-PEG-PAMA/pDNA polyplex micelle (about 1 order of magnitude increase in transfection efficiency), whereas it showed an appreciable decrease in the transfection efficiency in the presence of NR (5 μM) for the Lac-PEG-PSAO-PAMA/pDNA polyplex micelles and the B-PEI/pDNA polyplex. This is in line with the assumption that the Lac-PEG-PSAO-PAMA/pDNA polyplex micelles may be equipped with an endosome escaping function due to the unprotonated pH-responsive PSAO segment in the polyplex micelles.

A significant decrease in the transfection efficiency of the Lac-PEG-PSAO-PAMA/pDNA polyplex micelles was observed in the presence of ASF, consistent with the results of cellular uptake, as shown in Figure 9. Alternatively, no effect of ASF was observed even for the Lac-PEG-PAMA/pDNA polyplex micelle, suggesting that the endosomal escape may be the most critical barrier to intracellular gene delivery by Lac-PEG-PAMA/pDNA polyplex micelle. Thus, it may be reasonable to conclude that an appreciable fraction of the Lac-PEG-PSAO-PAMA/pDNA polyplex micelles is taken up into HuH-7 cells through the ASGP receptor-mediated endocytosis process mediated by the cluster of the large number of lactose moieties on the surface of the polyplex micelles, followed by the effective disruption of the endosome by the buffer effect of the unprotonated pH-responsive PSAO segment in the polyplex micelles.

It is well-known that components of the serum may interact with the polyplex to induce its structure change, resulting in decreasing transfection efficiency. Thus, we examined the effect of the 20% serum preincubation for 6 h on the transfection efficiency of Lac-PEG-PSAO-PAMA/pDNA, Lac-PEG-PAMA/pDNA polyplex micelles, and B-PEI/pDNA polyplexes. As shown in Figure 12, 1 order of magnitude decrease in the transfection efficiency was observed for B-PEI/pDNA polyplexes after preincubation with 20% serum probably due to the nonspecific interaction of the cationic polyplexes with negatively charged biomacromolecules, inducing the decrease in the cellular uptake. In a sharp contrast, the polyplex micelle sytems still retained sufficient transfection efficiency toward HuH-7 cells even after preincubation with 20% serum. The almost neutral surface charge ($\zeta \sim +5$ mV in Table 1) of the Lac-PEG-PSAO-PAMA/pDNA polyplex micelles with the highly lactosylated PEG outer shell surrounding the PIC core and the PSAO inner shell may induce the micelles to tolerate serum components, allowing the cellular specific interaction through ASGP receptor-mediated endocytosis to retain efficiency even after the serum preincubation.

CONCLUSIONS

In conclusion, this study demonstrates the pH-responsive nature of novel three-layered polyplex micelles composed of a lactosylated-PEG-PSAO-PAMA triblock copolymer and pDNA, aimed at the development of a targetable and endosome-disruptive gene delivery system. The Lac-PEG-PSAO-PAMA triblock copolymer bearing a PAMA segment as the DNA-condensing polyamine and a PSAO segment as the pH-responsive polyamine was successfully synthesized. The Lac-PEG-PSAO-PAMA triblock copolymer, thus prepared, spontaneously associated with pDNA to form three-layered polyplex micelles with a PAMA/pDNA PIC core, a free PSAO inner shell, and a lactosylated PEG outer shell, as confirmed by ^{1}H NMR spectroscopy. Under physiological conditions, the Lac-PEG-PSAO-PAMA/pDNA polyplex micelles prepared at an N/P ratio above 3 were found to be able to condense pDNA (EtBr assay), thus forming polyplex micelles with a relatively small size (< 150 nm, DLS measurements), and an almost neutral surface charge ($\zeta \sim +5$ mV, zeta-potential measurements). The Lac-PEG-PSAO-PAMA/pDNA polyplex micelle formed at N/P = 3 exhibited a pH-induced size variation (pH = 7.4, 132.6 nm → pH = 4.0, 181.8 nm) corresponding to the conformational changes (globule-rod transition) in the uncomplexed PSAO chain in response to pH. The swelling of the free PSAO inner shell is likely to occur in this process while retaining the condensed PIC core composed of the PAMA segment and pDNA. The fluorescence microscopic observation revealed that the interaction of the polyplex micelle entrapping FITC-labeled pDNA with HuH-7 cells was significantly reduced in the presence of ASF compared to the condition without ASF, suggesting that ASGP receptor-mediated endocytosis would be a major route of the cellular uptake of the Lac-PEG-PSAO-PAMA/pDNA polyplex micelles. Furthermore, the Lac-PEG-PSAO-PAMA/pDNA polyplex micelles exhibited more efficient transfection ability than Lac-PEG-PSAO/pDNA and Lac-PEG-PAMA/pDNA polyplex micelles. Presumably, the Lac-PEG-PSAO-PAMA/pDNA polyplex micelles might have an endosomal escape function, and thus, hydroxychloroquine as an endosomolytic agent was not required to observe appreciable transfection. Several important factors are likely to be synergistically involved in the pronounced transfection efficiency of the Lac-PEG-PSAO-PAMA/pDNA polyplex micelles, such as minimal interaction with serum proteins, enhancement of the cellular uptake through ASGP receptor-mediated endocytosis, and effective transport to the cytoplasm from the endosomal compartment (endosomal escape). Therefore, the polyplex micelle composed of the ABC triblock copolymer, thus described here, would be a promising vector for smart gene delivery.

ACKNOWLEDGMENT

This work was supported by the Core Research for Evolutional Science and Technology (CREST) from the Japan Science and Technology Agency [JST]. We thank Professor Dr. Teiji Tsuruta for helpful comments on the preparation of the manuscript and Hiroshi Ogawa for the excellent experimental support.

Supporting Information Available: Other experimental procedures and results including synthesis of PEGs, the ^{1}H NMR spectrum of polyplex micelles at pD 4.0, and the MTT assay. This material is available free of charge via the Internet at http://pubs.acs.org.

LITERATURE CITED

(1) Yang, Y., Li, Q., Ertl, H. C., and Wilson, J. M. (1995) Cellular and humoral immune response to viral antigens create barrier to lung-directed gene therapy with recombinant adenoviruses. *J. Virol. 69*, 2004−2015.

(2) Yang, Y., Li, Q., Ertl, H. C., and Wilson, J. M. (1994) MHC class I-restricted cytotoxic T lymphocytes to viral antigens destroy hepatocytes in mice infected with E1-deleted recombinant adenoviruses. *Immunity 1*, 433−442.

(3) Gunter, K. C., Khan, A. S., and Noguchi, P. D. (1993) The safety of retroviral vectors. *Hum. Gene Ther. 4*, 643−645.

(4) Wakebayashi, D., Nishiyama, N., Itaka, K., Miyata, K., Yamasaki, Y., Harada, A., Koyama, H., Nagasaki, Y., and Kataoka, K. (2004) Polyion complex micelles of pDNA with acetal-poly(ethylene glycol)-poly(2-(dimethylamino)ethyl methacrylate) block copolymer as the gene carrier system: physicochemical properties of micelles relevant to gene transfection efficacy. *Biomacromolecules 5*, 2128−2136.

(5) Itaka, K., Yamauchi, K., Harada, A., Nakamura, K., Kawaguchi, H., and Kataoka, K. (2003) Polyion complex micelles from plasmid DNA and poly(ethylene glycol)-poly(L-lysine) block copolymer as serum-tolerable polyplex system: physicochemical properties of micelles relevant to gene transfection efficiency. *Biomaterials 24*, 4495−4506.

(6) Itaka, K., Yamauchi, K., Harada, A., Nakamura, K., Kawaguchi, H., and Kataoka, K. (2002) Evaluation by fluorescence resonance energy transfer of the stability of nonviral gene delivery vectors under physiological conditions. *Biomacromolecules 3*, 841−845.

(7) Harada-Shiba, M., Yamauchi, K., Harada, A., Takamisawa, I., Shimokado, K., and Kataoka, K. (2002) Polyion complex micelles as vectors in gene therapy-pharmacokinetics and in vivo gene transfer. *Gene Therapy 9*, 407−417.

(8) Kataoka, K., Harada, A., Wakebayashi, D., and Nagasaki, Y. (1999) Polyion complex micelles with reactive aldehyde groups on their surface from plasmid DNA and end-functionalized charged block copolymers. *Macromolecules 32*, 6892−6894.

(9) Katayose, K., and Kataoka, K. (1998) Remarkable increase in nuclease resistance of plasmid DNA through supramolecular assembly with poly(ethylene glycol)-poly(L-lysine) block copolymer. *J. Pharm. Sci. 87*, 160−163.

(10) Katayose, S., and Kataoka, K. (1997) Water-soluble polyion complex associates of DNA and poly(ethylene glycol)-poly(L-lysine) block copolymer. *Bioconjugate Chem. 8*, 702−707.

(11) Wakebayashi, D., Nishiyama, N., Yamasaki, Y., Itaka, K., Kanayama, N., Harada, A., Nagasaki, Y., and Kataoka, K. (2004) Lactose-conjugated polyion complex micelles incorporating plasmid DNA as a targetable gene vector system: their preparation and gene transfecting efficiency against cultured HepG2 cells. *J. Control. Release 95*, 653−664.

(12) van de Wetering, P., Cherng, J. Y., Talsma, H., Crommelin, D. J. A., and Hennink, W. E. (1998) 2-(Dimethylamino)ethyl methacrylate based (co)polymers as gene transfer agents. *J. Control. Release 53*, 145−153.

(13) Cherng, J. Y., Van de Wetering, P., Talsma, H., Crommelin, D. J. A., and Hennink, W. E. (1996) Effect of size and serum proteins on transfection efficiency of poly ((2-dimethylamino)ethyl methacrylate)-plasmid nanoparticles. *Pharm. Res. 13*, 1038−1042.

(14) Brown, M. D., Schatzlein, A. G., and Uchegbu, I. F. (2001) Gene delivery with synthetic (non viral) carriers. *Int. J. Pharm. 229*, 1−21.

(15) Nishikawa, M., and Huang, L. (2001) Nonviral vectors in the new millennium: delivery barriers in gene transfer. *Hum. Gene Ther. 12*, 861−870.

(16) Lloyd, J. B. (2000) Lysosome membrane permeability: implications for drug delivery. *Adv. Drug Deliv. Rev. 41*, 189−200.

(17) Gruenberg, J. (2001) The endocytic pathway: a mosaic of domains. *Nat. Rev.: Mol. Cell. Biol. 2*, 721−730.

(18) Clague, M. J. (1998) Molecular aspects of the endocytic pathway. *Biochem. J. 336*, 271−282.

(19) Mukherjee, S., Ghosh, R. N., and Maxfield, F. R. (1997) Endocytosis. *Physiol. Rev. 77*, 759−803.

(20) Duncan, R. (1992) Drug-polymer conjugates: potential for improved chemotherapy. *Anti-Cancer Drugs 3*, 175−210.

(21) Boussif, O., Lezoualc, F., Zanta, M. A., Mergny, M. D., Scherman, D., Demeneix, B., and Behr, J. P. (1995) A versatile vector for gene

and oligonucleotide transfer into cells in culture and in vivo: polyethylenimine. *Proc. Natl. Acd. Sci. U.S.A. 92*, 7297−7301.
(22) Kabanov, A. V., Bronich, T. K., Kabanov, V. A., Yu, K., and Eisenberg, A. (1998) Soluble stoichiometric complexes from poly(*N*-ethyl-4-vinylpyridinium) cations and poly(ethylene oxide)-*block*-polymethacrylate anions. *Macromolecules 29*, 6797−6802.
(23) Fukushima, S., Miyata, K., Nishiyama, N., Kanayama, N., Yamasaki, Y., and Kataoka, K. (2005) PEGylated polyplex micelles from triblock catiomers with spatially ordered layering of condensed pDNA and buffering units for enhanced intracellular gene delivery. *J. Am. Chem. Soc. 127*, 2810−2811.
(24) Nagasaki, Y., Luo, L. B., Tsuruta, T., and Kataoka, K. (2001) Novel pH-sensitive poly(silamine) hydrogel microsphere possessing a stable skin layer. *Macromol. Rapid Commun. 22*, 1124−1127.
(25) Luo, L. B., Kato, M., Tsuruta, T., Kataoka, K., and Nagasaki, Y. (2000) Stimuli-sensitive polymer gels that stiffen upon swelling. *Macromolecules 33*, 4992−4994.
(26) Nagasaki, Y., Kazama, K., Honzawa, E., Kato, M., Kataoka, K., and Tsuruta, T. (1996) A hydrogel with rubber elasticity transition. *Macromol. Symp. 109*, 27−40.
(27) Nagasaki, Y., Kazama, K., Honzawa, E., Kato, M., Kataoka, K., and Tsuruta, T. (1995) Rubber elasticity transition of poly(silamine) induced by ionic interactions. *Macromolecules 28*, 8870−8871.
(28) Nagasaki, Y., Honzawa, E., Kato, M., and Kataoka, K. (1994) Novel stimuli-sensitive telechelic oligomers. pH and temperature sensitivities of poly(silamine) oligomers. *Macromolecules 27*, 4848−4850.
(29) Nagasaki, Y., Honzawa, E., Kato, M., Kihara, Y., and Tsuruta, T. (1992) Novel synthesis of a macromonomer having organosilyl and amino groups. *J. Macromol. Sci., Pure Appl. Chem. A29*, 457−470.
(30) van de Wetering, P., Schuurmans-Nieuwenbroek, N. M. E., Hennink, W. E., and Storm, G. (1999) Comparative transfection studies of human ovarian carcinoma cells in vitro, ex vivo and in vivo with poly(2-(dimethylamino)ethyl methacrylate)-based polyplexes. *J. Gene Med. 1*, 156−165.
(31) Cherng, J. Y., Talsma, H., Verrijik, R., Crommelin, D. J., and Hennink, W. E. (1999) The effect of formulation parameters on the size of poly-((2-dimethylamino)ethyl methacrylate)-plasmid complexes. *Eur. J. Pharm. Biopharm. 47*, 215−224.
(32) Nagasaki, Y., Sato, Y., and Kato, M. (1997) A novel synthesis of ssemitelechelic functional poly(methacrylate)s through an alcoholate-initiated polymerization. Synthesis of poly[2-(N,N-diethylaminoethyl) methacrylate] macromonomer. *Macromol. Rapid Commun. 18*, 827−835.
(33) Kitano, H., Shoda, K., and Kosaka, A. (1995) Galactose-containing amphiphiles prepared with a lipophilic radical initiator. *Bioconjugate Chem. 6*, 131−134.
(34) Hashida, M., Takemura, S., Nishikawa, M., and Takakura, Y. (1998) Targeted delivery of plasmid DNA complexed with galactosylated poly(L-lysine). *J. Controlled Release 53*, 301−310.
(35) Stockert, R. J. (1995) The asialoglycoprotein receptor: relationships between structure, function, and expression. *Physiol. Rev. 75*, 591−609.
(36) Zanta, M. A., Boussif, O., Adib, A., and Behr, J. P. (1997) In vitro gene delivery to hepatocytes with galactosylated polyethylenimine. *Bioconjugate Chem. 8*, 839−844.
(37) Plank, C., Mechter, K., Szoka, F. C., Jr., and Wagner, E. (1996) Activation of the complement system by synthetic DNA complexes: a potential barrier for intravenous gene delivery. *Hum. Gene Ther. 7*, 1437−1446.
(38) Uherek, C., Fominaya, J., and Wels, W. (1998) A modular DNA carrier protein based on the structure of diphtheria toxin mediates target cell-specific gene delivery. *J. Biol. Chem. 273*, 8835−8841.

BC050364M

Available online at www.sciencedirect.com
SCIENCE DIRECT®
Journal of Controlled Release 111 (2006) 368–370
journal of controlled release
www.elsevier.com/locate/jconrel

Rapid communication

Organic–inorganic hybrid-nanocarrier of siRNA constructing through the self-assembly of calcium phosphate and PEG-based block aniomer

Yoshinori Kakizawa [a], Sanae Furukawa [a], Atushi Ishii [b,c], Kazunori Kataoka [c,d,e,*]

[a] *Biomaterials Center, National Institute for Materials Science, 1-1 Namiki, Tsukuba, Ibaraki 305-0044, Japan*
[b] *NanoCarrier Co., 5-4-19 Kashiwanoha, Kashiwa, Chiba 277-0882, Japan*
[c] *Department of Materials Engineering, Graduate School of Engineering, The University of Tokyo, 7-3-1 Hongo, Bunkyo-ku, Tokyo 113-8656, Japan*
[d] *Division of Clinical Biotechnology, Center for Disease Biology and Integrative Medicine, Graduate School of Medicine, The University of Tokyo, 7-3-1 Hongo, Bunkyo-ku, Tokyo 113-0033, Japan*
[e] *Center for NanoBio Integration, The University of Tokyo, 7-3-1 Hongo, Bunkyo-ku, Tokyo, 113-8656, Japan*

Received 30 October 2005; accepted 16 January 2006
Available online 28 February 2006

Abstract

The development of siRNA delivery systems is a major key for practical RNA therapy that holds promise for the treatment of life-threatening human diseases, yet there still exists significant difficulties in their construction because of the various requirements including high transfection efficacy, tolerability in the biological medium, and low toxicity. Here we report the novel preparation route of organic–inorganic hybrid-nanocarriers entrapping siRNA based on the self-assembly of the block aniomer, poly(ethylene glycol)-*block*-poly(methacrylic acid), with calcium phosphate crystals. The nanocarriers have diameters in the range of several hundreds of nanometers and revealed excellent colloidal stability due to the steric stabilization effect of the PEG palisade. The biological activity of siRNA loaded in nanocarriers was assessed using 293 cells stably expressing luciferase gene, showing the remarkably high gene silencing-efficacy without the use of any adjuvant molecules such as chroloquin. Further advantage of the system is the serum tolerability, which is of a critical issue in in vivo application.

Short interfering RNA (siRNA) that mediates gene-silencing phenomena of RNA interference (RNAi) needs a carrier system to exert biological activity, especially, for in vivo application [1]. Some lipid- and polymer-based systems are available for the in vitro application of siRNA, yet they often have drawbacks including a low stability in a serum-containing medium and significant cytotoxicity. From the standpoint of developing a safe and serum-tolerable carrier system, the calcium phosphate (CaP) co-precipitation method is of interest [2]. To control the growth of CaP, that is the determining factor for the transfection efficacy, a novel concept has recently been introduced by our group based on the self-assembly of poly(ethylene glycol)-*block*-poly(aspartic acid) block copolymers (PEG-P(Asp)) with CaP to form the narrowly distributed hybrid nanoparticles covered with PEG palisades [3].

siRNA-entrapped PEG-P(Asp)/CaP hybrid nanoparticles indeed revealed an appreciable gene silencing in a cultured cell line [4]. Nevertheless, the requirement of chroloquin, a reagent facilitating endosomal-escape, impedes the wide applicability of this method. Herein, we overcome this critical issue using the newly designed system of siRNA-entrapped CaP nanoparticles. The strategy is to incorporate the molecular units facilitating endosomal-escape directly into the block copolymer structure. In this regard, poly(methacrylic acid) (PMA) was selected as the polyanion unit in the block copolymer. PMA undergoes a conformational transition at pH 4–6, which almost corresponds to the endosomal pH, to adopt a more hydrophobic conformation as compared to neutral pH, thus expected to have an increased interaction with the endosomal membrane in order to perturb its structure to facilitate escape of the nanoparticles into the cytoplasm [5]. Here, two different compositions of the poly(ethylene glycol)-*block*-poly(methacrylic acid) (PEG-PMA) were used for the nanoparticle formation entrapping siRNA. PEG-PMA1 has a PEG segment with the molecular weight (Mw) of 7800 and the PMA segment with the Mw of

* Corresponding author. Department of Materials Engineering, Graduate School of Engineering, The University of Tokyo, 7-3-1 Hongo, Bunkyo-ku, Tokyo 113-8656, Japan.
E-mail address: kataoka@bmw.t.u-tokyo.ac.jp (K. Kataoka).

0168-3659/$ - see front matter © 2006 Elsevier B.V. All rights reserved.
doi:10.1016/j.jconrel.2006.01.004

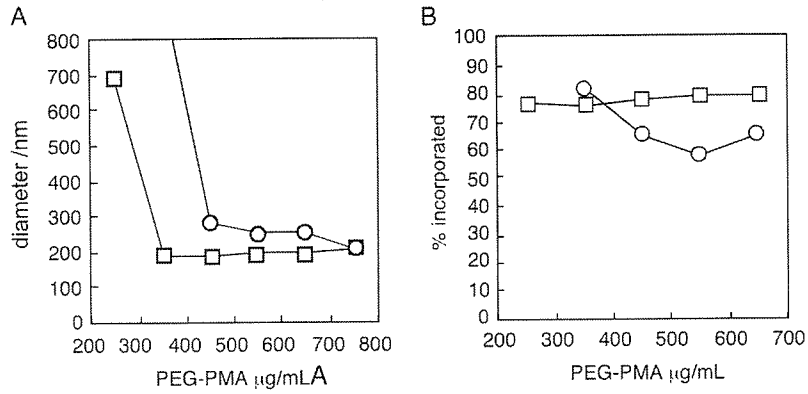

Fig. 1. Physicochemical characterization of nanoparticles composed of PEG-PMA1 (□) and PEG-PMA2 (○). (A) Size of the nanoparticles entrapping siRNA determined by DLS measurements. (B) Percentage of siRNA loaded in the nanoparticles formed at varying PEG-PMA concentrations.

2000, while the Mw of the PEG and PMA segments of PEG-PMA2 are 7500 and 15,500, respectively.

The diameters of the nanoparticles formed in the presence of the PEG-PMAs are determined by dynamic light scattering measurements [6,7]. Fig. 1A shows the change in diameters of nanoparticles with varying concentrations of PEG-PMAs at 3.0 mM phosphate. A similar trend was observed for PEG-PMA1 and PEG-PMA2, and the stable dispersion of nanoparticles was obtained over certain concentrations; 350 μg/mL for PEG-PMA1 and 450 μg/mL for PEG-PMA2. Diameters above these critical concentrations of PEG-PMA were about 180–200 and 200–280 nm for PEG-PMA1 and PEG-PMA2, respectively. It is noteworthy that at those concentrations no precipitation of CaP was observed 24 h after the mixing of Ca/siRNA and phosphate/PEG-PMA solution. The polydispersity indices of the nanoparticles were below 0.1 for PEG-PMA1, suggesting a unimodal distribution, while the values were slightly higher (0.12–0.15) for PEG-PMA2. The zeta potential of nanoparticles composed of 450 μg/mL of PEG-PMA1 or PEG-PMA2 was almost zero, −1.50±0.36 and −0.439±0.118 mV, respectively, indicating that the colloidal stability of the nanoparticles is caused by the PEG palisades with the steric repulsion effect. The incorporation efficacy of siRNA in the nanoparticles determined by the centrifugation method was around 80% for PEG-PMA1 and 60–80% for PEG-PMA2 [8] (Fig. 1B).

In order to investigate RNAi activity of siRNA incorporated in the nanoparticles, we have established a 293 cell line stably expressing the GL3-luciferase gene and estimated the degree of gene silencing using the siRNA targeting GL3-luciferase gene [9–11] . Fig. 2A shows the effect of the PEG-PMA concentrations on the RNAi activity of the siRNA-loaded nanoparticles, expressed as the relative inhibition activity to the control (non-silencing) siRNA. PEG-PMA1 showed no remarkable RNAi activity (■), while the PEG-PMA2 system (●) achieved a gene silencing down to 20% of the control (80% inhibition) in the polymer concentration range of 450 to 550 μg/mL. The

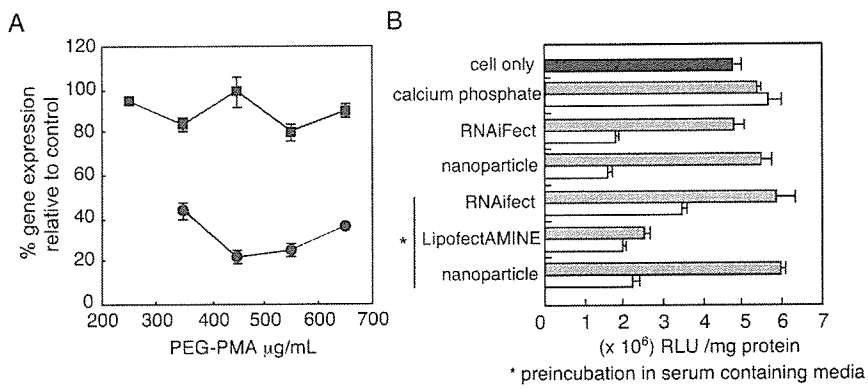

Fig. 2. Biological activity of siRNA incorporated in nanoparticles. (A) RNA interference by siRNA incorporated in nanoparticles formed at various concentrations of PEG-PMAs. GL3 luciferase gene expression in 293 cells was inhibited by nanoparticles composed of PEG-PMA1 (■) and PEG-PMA2 (●). Results are shown as the percentage to the control expression of cells treated with nanoparticles entrapping non-silencing siRNA. (B) RNA interference by siRNA using various transfection reagents. Grey bars indicate GL3 luciferase gene expressions in 293 cells treated with non-silencing control siRNA, and white bars indicate those treated with GL3 siRNA. The nanoparticle samples are composed of calcium phosphate and PEG-PMA2 formed at 450 μg/mL. For the preincubation study (*), DMEM containing 20% FCS was added to an equal amount of nanoparticle or lipoplex solutions and incubated at 37 °C for 30 min prior to the transfection. In the calcium phosphate method, the transfection was performed under the same condition as the nanoparticle except in the absence of PEG-PMA. The concentrations of siRNA and calcium ion in all the experiments were 125 nM and 6.25 mM, respectively.

reason for the presence of the maximum transfection efficacy in terms of the PEG-PMA concentration is not yet clear, however, nanoparticles with smaller diameters seem to be more efficient than the larger CaP/PEG-PMA complex or precipitate formed at the lower PEG-PMA concentration. For example, at 250 μg/mL PEG-PMA1, at which a large precipitate was formed, no silencing was recognized. The siRNA concentration dependency was evaluated using the sample solutions prepared by dilution of the stock nanoparticle solution formed at 450 μg/mL of PEG-PMA2 and 2.5 μM of siRNA. The significant inhibition was observed at a concentration as low as 6.7 nM (45% inhibition) and reached a plateau value around 25 nM (80% inhibition).

To clarify the advantages of this system, the transfection efficacy was further compared with other transfection reagents and the conventional calcium phosphate method (Fig. 2B). Under the experimental conditions, the hybrid nanoparticles formed at 450 μg/mL of PEG-PMA showed transfection efficacy similar to RNAiFect. Worth noting is that the nanoparticles are more efficient in silencing than RNAiFect at the more physiologically relevant conditions: Preincubation in the DMEM containing 10% FCS was performed for 30 min prior to the transfection (*—marked conditions in Fig. 2B). Upon serum pre-incubation, the GL3 luciferase expression relative to the control increased from 36% to 58% in the case of RNAiFect, while the increase is only 29% to 35% for the hybrid nanoparticle system. Another type of lipid-based transfection reagent, lipofectAMINE, showed a non-specific effect in the serum-containing medium, which resulted in a significantly reduced luciferase activity even using the controlled non-silencing siRNA, presumably due to the toxicity. Tolerability to the serum is crucial when considering the in vivo application of the carrier system, especially, in the case of the systemic administration. Indeed, the in vivo application of a conventionally available cationic-lipid system is reported to be hampered in the serum-containing medium [12]. Furthermore, no significant activity of siRNA was observed for the calcium phosphate crystal prepared in the absence of PEG-PMA, indicating the necessity of the block copolymer for the improved transfection activity.

In summary, we demonstrated a highly efficient transfection of siRNA to cultured mammalian cells using nano-sized calcium phosphate crystals with appreciable serum tolerability. This nano-particulate siRNA carrier possessing a biocompatible PEG palisade and a pH-responsive moiety of PMA to facilitate endosomal escape may have a promising utility in RNAi research directed toward disease treatment.

Acknowledgements

This work was supported in part by the Core Research for Evolution of Science and Technology (CREST), Japan Science and Technology Corporation (JST) and by the Project on Material Development for Innovative Nano-Drug Delivery Systems, The Ministry of Education, Culture, Sports, Science and Technology, Japan (MEXT).

References

[1] F. Simeoni, M.C. Morris, F. Heitz, G. Divita, Nucleic Acids Res. 31 (2003) 2717–2724;
D.R. Sørensen, M. Leirdal, M. Sioud, J. Mol. Biol. 327 (2003) 761–766.
[2] C. Chen, H. Okayama, Mol. Cell. Biol. 7 (1987) 2745–2752;
H. Tolou, Anal. Biochem. 215 (1993) 156–158.
[3] Y. Kakizawa, K. Kataoka, Langmuir 18 (2002) 4539–4543.
[4] Y. Kakizawa, S. Furukawa, K. Kataoka, J. Control. Release 97 (2004) 345–356.
[5] M. Mandel, J.C. Leyte, M.G. Standhouder, J. Phys. Chem. 71 (1967) 603–612;
A.F. Olea, H. Rosenbluth, J.K. Thomas, Macromolecules 32 (1999) 8077–8083.
[6] The nanoparticles were prepared as follows: A solution of 2.5 M $CaCl_2$ was added to a solution of siRNA in a buffer (1 mM Tris–HCl, 0.1 mM EDTA, pH 7.6) to a final volume (Ca^{2+} 250 mM, siRNA 74 μg/mL). One volume of this 2× Ca/siRNA solution was quickly added to an equal volume of 2× Hepes/phosphate/PEG-PMA solution (140 mM NaCl, 50 mM HEPES, 6.0 mM Na_2HPO_4, PEG-PMA, pH 7.1). The mixed solutions were vigorously stirred by a vortex mixer for a few seconds and incubated at 37 °C for 24 h.
[7] D.E. Koppel, J. Chem. Phys. 57 (1972) 4814–4820.
[8] siRNA content was determined as follows: The sample solutions (200 μL) were centrifuged at 15000 ×*g* for 30 min to precipitate the nanoparticles. Supernatants (100 μL) were carefully removed to determine siRNA concentration by absorbance at 260 nm. The percentage of the loaded siRNA was calculated by subtracting the siRNA concentration in the supernatant from the total concentration.
[9] siRNA targeting GL3-luciferase gene, antisense sequence; 5′-UCGAA GUACUCAGCGUAAGdTdT-3′, sense sequence; 5′-CUUACGCUGA GUACUUCGAdTdT-3′, control (non-silencing) siRNA: antisense sequence; 5′-UUCUCCGAACGUGUCACGUdTdT-3′, sense sequence; 5′-ACGUGACACGUUCGGAGAAdTdT-3′).
[10] S.M. Elbashir, J. Harboth, W. Lendeckel, A. Yalcin, K. Weber, T. Tuschl, Nature 11 (2001) 494–498.
[11] The 293 cell line stably expressing GL3-luciferase gene was established using Flp-In system (Invitrogen) according to the manufacturer's protocol. The cells were plated at the density of ~8×10^3 cells/well in a 96 well plate and grown overnight in medium containing 10% FCS. Before transfection, the medium was removed and 50 μL of fresh medium containing 20% FCS was added to each well. The stock nanoparticle solutions (siRNA 2.5 μM) were diluted with DMEM to desired concentrations. Fifty microliters of the diluted sample solutions were added to each well and the cells were incubated at 37 °C for 42 h under 5% CO_2 atmosphere. Luciferase gene expression was measured using Luciferase assay kit from Promega. Protein concentration was determined by BCA protein assay kit from Pierce. For the commercially available transfection reagents, RNAiFect and LipofectAMINE, transfection experiments were performed following a protocol provided by the manufacturer. The conventional calcium phosphate co-precipitation method was performed as Jordan et al. reported (Jordan, M.; Schallhorn, A.; Wurm, F. M. Nucleic Acids Res. 1996, 24, 596–601).
[12] A. Chonn, S.C. Semple, P.R. Cullis, J. Biol. Chem. 267 (1992) 18759–18765;
S. Li, W.C. Tseng, D.B. Stolz, S.P. Wu, S.C. Watkins, L. Huang, Gene Ther. 6 (1999) 585–594.

DOI: 10.1002/cmdc.200600008

A PEG-Based Biocompatible Block Catiomer with High Buffering Capacity for the Construction of Polyplex Micelles Showing Efficient Gene Transfer toward Primary Cells

Naoki Kanayama,[a, d] Shigeto Fukushima,[a, c] Nobuhiro Nishiyama,*[b] Keiji Itaka,[b] Woo-Dong Jang,[a] Kanjiro Miyata,[a] Yuichi Yamasaki,[a, d] Ung-il Chung,[b] and Kazunori Kataoka*[a, b, d]

Nonviral gene vectors from synthetic catiomers (polyplexes) are a promising alternative to viral vectors. In particular, many recent efforts have been devoted to the construction of biocompatible polyplexes for in vivo nonviral gene therapy. A promising approach in this regard is the use of poly(ethylene glycol) (PEG)-based block catiomers, which form a nanoscaled core–shell polyplex with biocompatible PEG palisades. In this study, a series of PEG-based block catiomers with different amine functionalities were newly prepared by a simple and affordable synthetic procedure based on an aminolysis reaction, and their utility as gene carriers was investigated. This study revealed that the block catiomers carrying the ethylenediamine unit at the side chain are capable of efficient and less toxic transfection even toward primary cells, highlighting critical structural factors of the cationic units in the construction of polyplex-type gene vectors. Moreover, the availability of the polyplex micelle for transfection with primary osteoblasts will facilitate its use for bone regeneration in vivo mediated by nonviral gene transfection.

Introduction

Gene therapy is a promising approach for the treatment of genetic and intractable diseases and for tissue engineering; however, its success still strongly depends on the development of useful gene vectors.[1] Recently, nonviral vectors based on the complexation of plasmid DNA (pDNA) with synthetic cationic polymers (catiomers) have attracted a great deal of attention as an alternative to viral vectors.[2–4] These vectors, the so-called polyplexes, are aimed toward both efficient transfection and decreased cytotoxicity.[5,6] In particular, there has recently been a strong impetus toward engineering the constituent catiomers to construct biocompatible polyplexes suitable for gene delivery in vivo.[2,5] A promising approach in this regard is the block copolymerization of catiomers with poly(ethylene glycol) (PEG) to obtain PEG-*block*-catiomers, as they spontaneously associate with pDNA to form polyplex micelles at the sub-100-nm scale with a dense and hydrophilic PEG palisade surrounding the polyplex core (Figure 1).[7–10] These polyplex micelles with PEG palisades showed high colloidal stability under physiological conditions and afforded appreciable levels of reporter-gene expression to various cell lines even after preincubation in a serum-containing medium.[7] Notably, the polyplex micelles demonstrated longevity in blood circulation,[11] offering the possibility of their use in systemic gene delivery. Nevertheless, a major obstacle to the successful application of this biocompatible nonviral vector system remains: the limited transfection efficacy toward primary cells.

Herein, we report a novel approach to obtain PEG-*block*-catiomers with remarkably high transfecting activity even toward primary cells, which are known to be sensitive to the toxicity induced by conventional polyplexes. The synthetic strategy for novel block catiomers is based on our unprecedented finding that the flanking benzyl ester groups of poly(β-benzyl L-aspar-

[a] Dr. N. Kanayama, S. Fukushima, Dr. W.-D. Jang, K. Miyata, Dr. Y. Yamasaki, Prof. Dr. K. Kataoka
Department of Materials Engineering
Graduate School of Engineering
The University of Tokyo
Tokyo 113-8656 (Japan)
Fax: (+81) 3-5841-7139
E-mail: kataoka@bmw.t.u-tokyo.ac.jp

[b] Dr. N. Nishiyama, Dr. K. Itaka, Prof. Dr. U.-i. Chung, Prof. Dr. K. Kataoka
Center for Disease Biology and Integrative Medicine
Graduate School of Medicine
The University of Tokyo, Tokyo 113-0033 (Japan)
Fax: (+81) 3-5841-7139
E-mail: nishiyama@bmw.t.u-tokyo.ac.jp

[c] S. Fukushima
R&D Division, Pharmaceuticals Group
Nippon Kayaku Co., Ltd. (Japan)

[d] Dr. N. Kanayama, Dr. Y. Yamasaki, Prof. Dr. K. Kataoka
Core Research for Evolutional Science and Technology (CREST), Japan Science and Technology Agency (JST) (Japan)

Supporting information for this article is available on the WWW under http://www.chemmedchem.org or from the author.

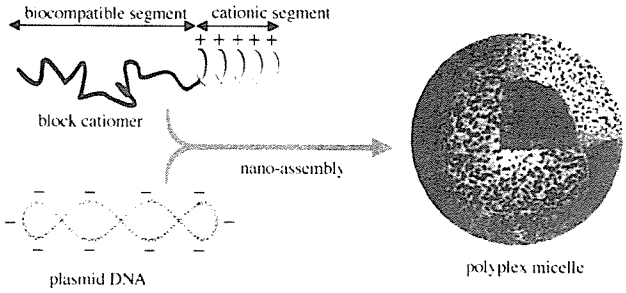

Figure 1. Formation of polyplex micelles through the electrostatic interaction between block catiomers and plasmid DNA.

tate) (PBLA) can undergo a quantitative aminolysis reaction with various polyamine compounds under mild anhydrous conditions at 40 °C, thus allowing the preparation of cationic polyaspartamides with different amine functionalities, yet with the same molecular weight and distribution (Scheme 1). In par-

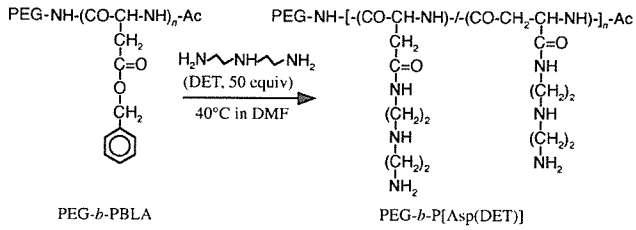

Scheme 1. Synthesis of PEG-*b*-P[Asp(DET)] block catiomer through the aminolysis of PEG-*b*-PBLA. DMF = *N*,*N*-dimethylformamide.

ticular, this study is focused on the unique properties of the ethylenediamine unit integrated into the polyaspartamide side chain. Notably, ethylenediamine is known to undergo a clear two-step protonation with a distinctive *gauche–anti* conformational transition as depicted in Scheme 2,[12] and is thus expected to provide an effective buffering function in the acidic en-

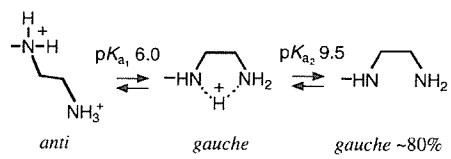

Scheme 2. Two-step protonation of the ethylenediamine unit with a distinctive *gauche–anti* conformational transition.

dosomal compartment (pH 5). It has been suggested that catiomers with a low pK_a value such as polyethylenimine could buffer endosomal acidification and cause an increase in osmotic pressure in the endosome, leading to the disruption of the endosomal membrane to facilitate polyplex transport into the cytoplasm (the so-called proton sponge effect[13]). Indeed, PEG-*block*-polyaspartamide with an ethylenediamine unit at the side chain (PEG-*b*-P[Asp(DET)]) showed a remarkably high transfection efficacy to various cancer cells as well as mouse primary osteoblast cells. Importantly, this block catiomer was found to have remarkably low toxicity, facilitating its use for in vivo gene therapy.

Results and Discussion

PEG-*b*-polyaspartamide carrying the *N*-(2-aminoethyl)aminoethyl group $-(CH_2)_2NH(CH_2)_2NH_2$ as the side chain (PEG-*b*-P[Asp(DET)]) was prepared by the aminolysis of PEG-*b*-PBLA in dry DMF at 40 °C for 24 h in the presence of a molar excess (50 equiv relative to benzyl groups) of diethylenetriamine (DET) (Scheme 1). The ^{1}H NMR spectrum of PEG-*b*-P[Asp(DET)] is shown in Figure 2, and the ^{13}C NMR spectrum is available in

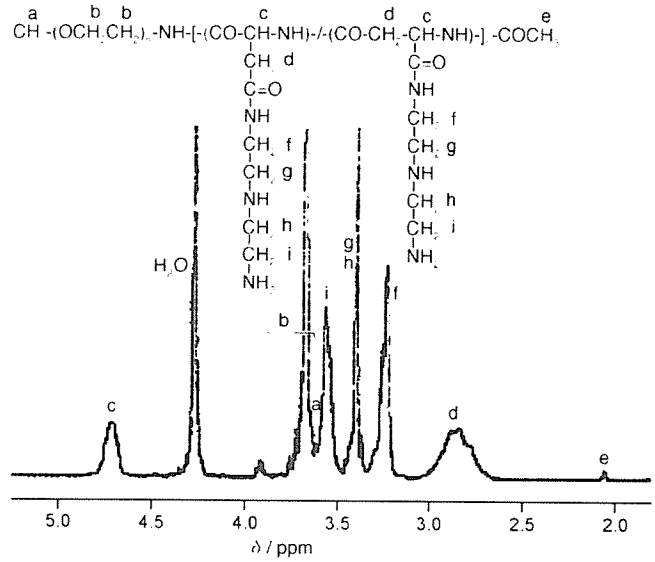

Figure 2. ^{1}H NMR spectrum of PEG-*b*-P[Asp(DET)] (solvent: D_2O, T = 80 °C); the polymer is in a salt form.

the Supporting Information. These data indicate that the aminolysis of the PBLA benzyl groups proceeded in a selective manner to the primary amine moiety of DET. Also, comparison of the integration ratio of the proton peaks (b and f–i) in Figure 2 reveals quantitative introduction of DET into the side chain of PBLA, and a unimodal molecular weight distribution of the obtained polymer was revealed by size-exclusion chromatography (SEC) measurement (Supporting Information). These results suggest a minimal occurrence of inter- or intrapolymer cross-linking by DET during aminolysis. Note that the peaks from the carbonyl and methylene groups of the aspartamide units in the ^{13}C NMR spectrum (Figure S1, Supporting Information) are split into two peaks, suggesting that the aminolysis of PBLA might induce intramolecular isomerization of the aspartamide units to form β-aspartamide. Figure 3 shows the time course of the aminolysis reaction of PBLA with DET, which was evaluated from the change in the ratio of the proton peak integration (f over b) in the ^{1}H NMR spectrum (Figure 2). This result indicates a fast and quantitative aminolysis of PBLA, which is in marked contrast to the lack of aminolysis with poly(γ-benzyl L-glutamate) (PBLG) under the same re-

